Boundary Layer Approximation

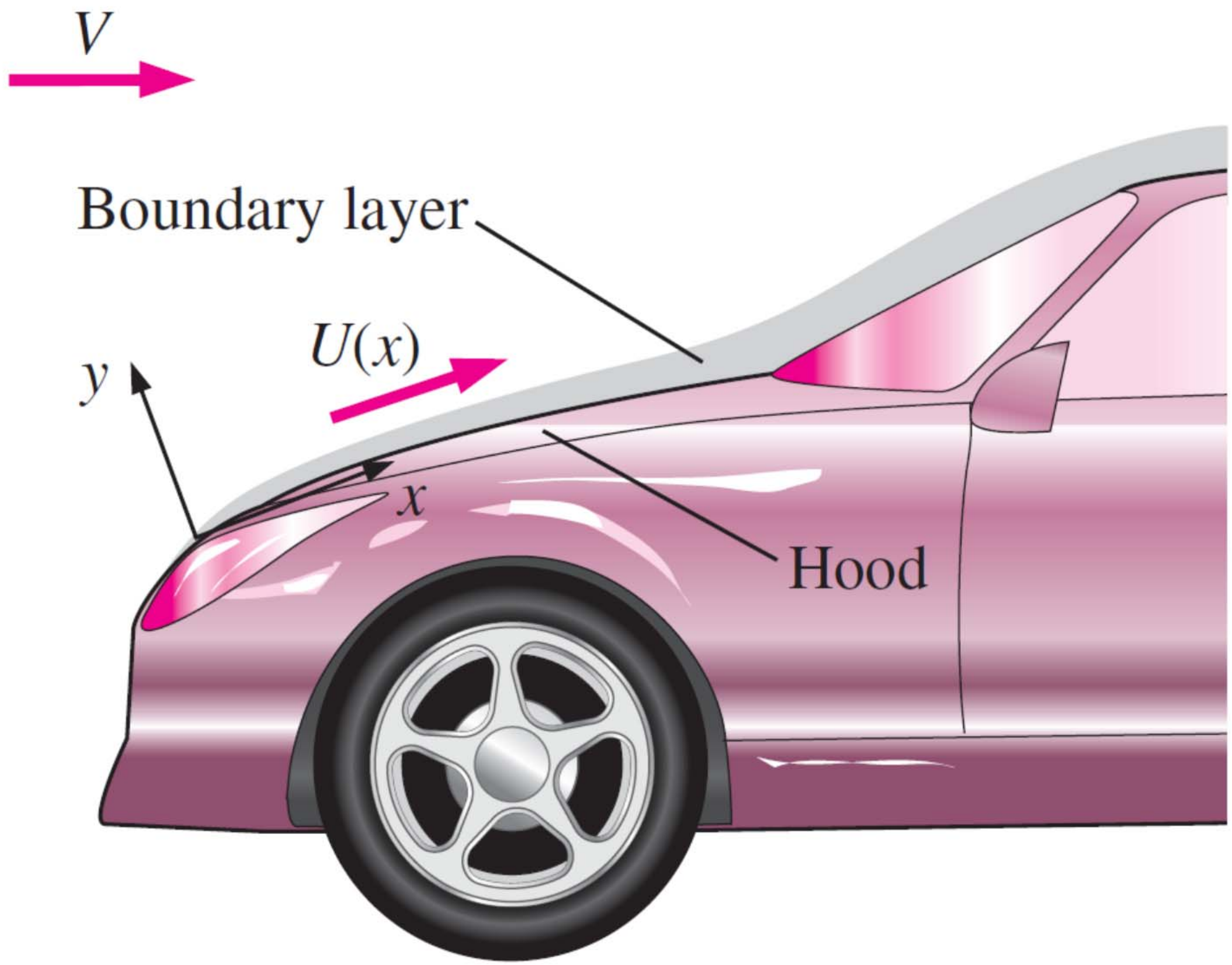

Boundary Layer Approximation

The boundary layer approximation bridges the gap between the Euler equation and the Navier–Stokes equation, and between the slip condition and the no-slip condition at solid walls.

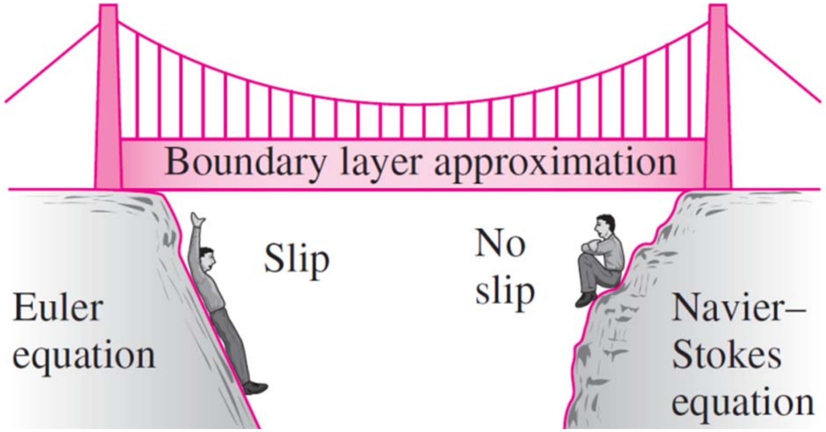

A major breakthrough in fluid mechanics occurred in 1904 when Ludwig Prandtl (1875–1953) introduced the **boundary layer approximation.**

<u>Two Zones</u>:
(i) inner flow region; called a *boundary layer* - a very thin region of flow near a solid wall where viscous forces and rotationality cannot be ignored.
(ii) Outer flow region; inviscid and/or irrotational.

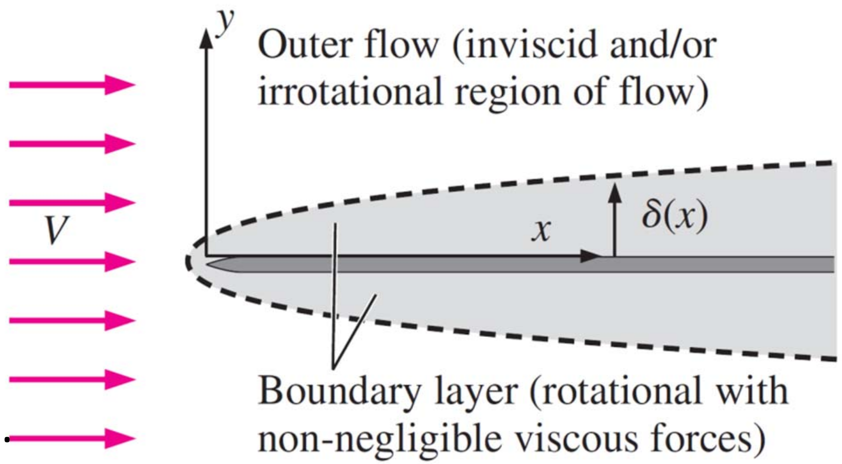

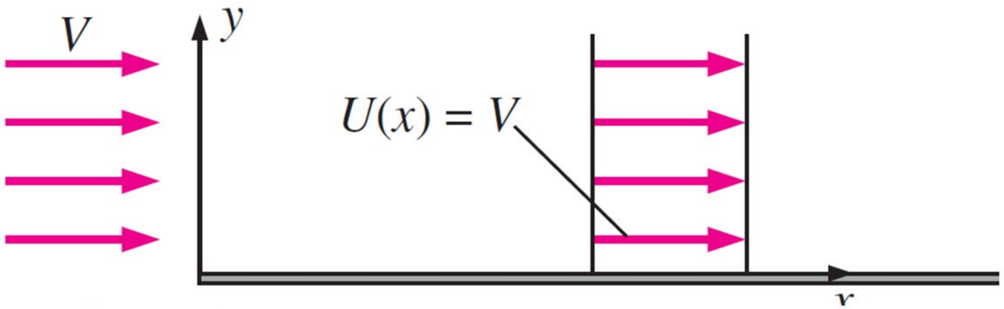

Inviscid Approximation

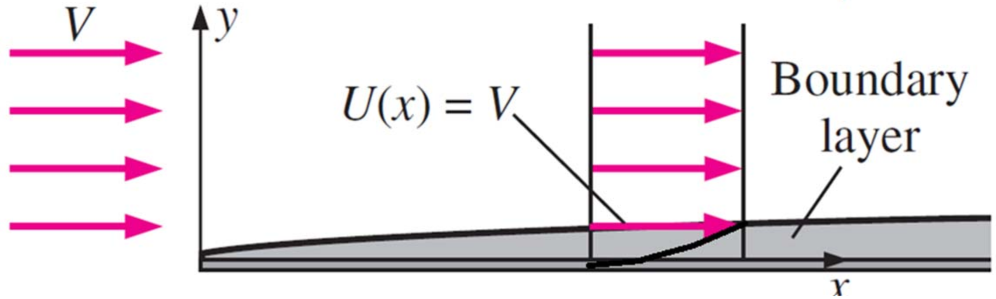

Viscous Approximation

The boundary layer is so thin that it does not affect the outer flow

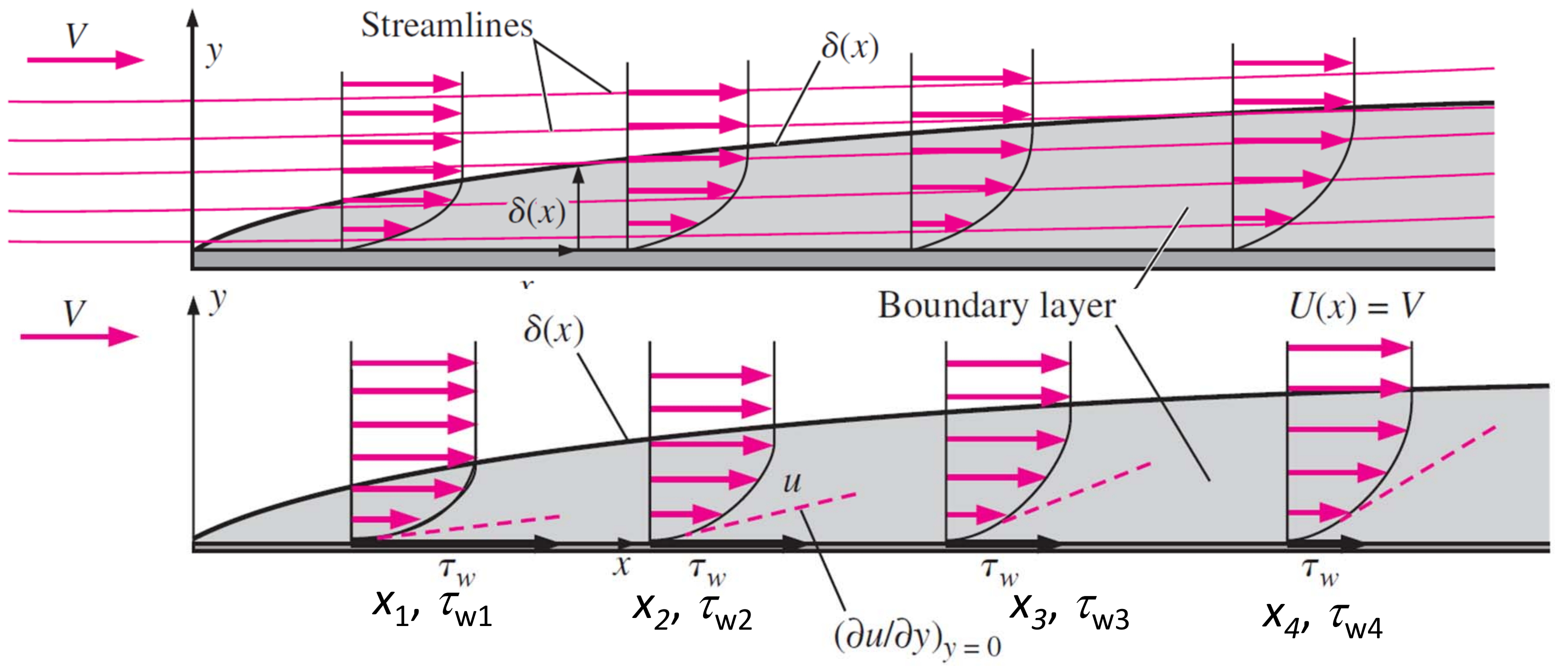

$\tau_{w1} > \tau_{w2} > \tau_{w3} > \tau_{w4}$

The key to successful application of the boundary layer approximation is the assumption that the boundary layer is very *thin*.

Boundary layer thickness, δ is usually defined as the distance away from the wall at which the velocity component parallel to the wall is 99% of the fluid speed outside the boundary layer.

Reynolds number based on plate local length: $\mathrm{Re}_x = \dfrac{Vx}{\nu}$

Reynolds number based on plate length: $\mathrm{Re}_L = \dfrac{VL}{\nu}$

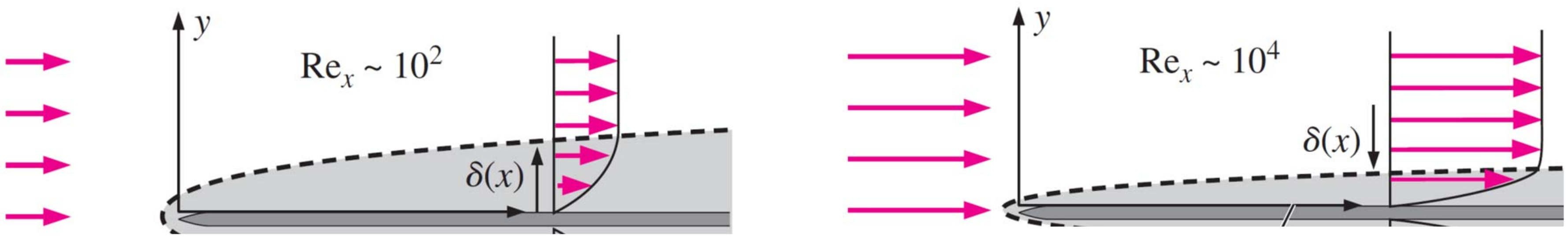

At a given *x*-location, the higher the Reynolds number, the thinner the boundary layer.

Boundary layer thickness varies with downstream distance as it grows downstream

DISPLACEMENT THICKNESS

Displacement thickness is the distance that a streamline just outside of the boundary layer is deflected away from the wall due to the effect of the boundary layer.

Applying conservation of mass to this control volume, the mass flow entering the control volume from the left (at x = 0) must equal the mass flow exiting from the right (at some arbitrary location x along the plate)

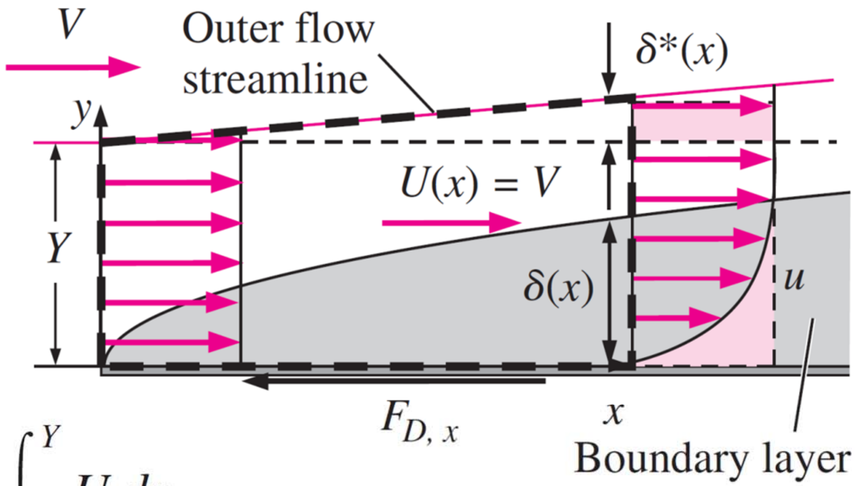

$$0 = \int_{CS} \rho \vec{V} \cdot \vec{n}\, dA = \underbrace{w\rho \int_0^{Y+\delta^*} u\, dy}_{\text{at location } x} - \underbrace{w\rho \int_0^{Y} U\, dy}_{\text{at } x = 0}$$

$$\int_0^Y (U - u)\, dy = U\delta^* \qquad \delta^* = \int_0^\infty \left(1 - \frac{u}{U}\right) dy$$

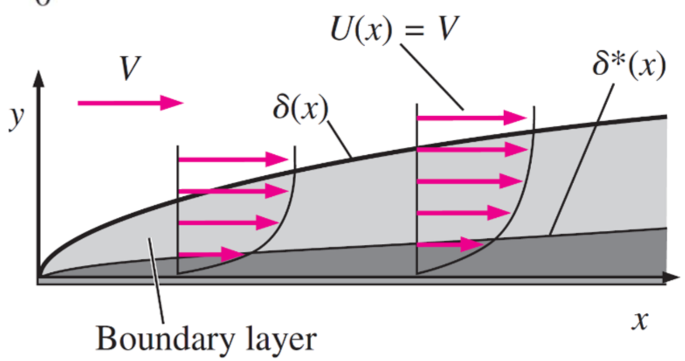

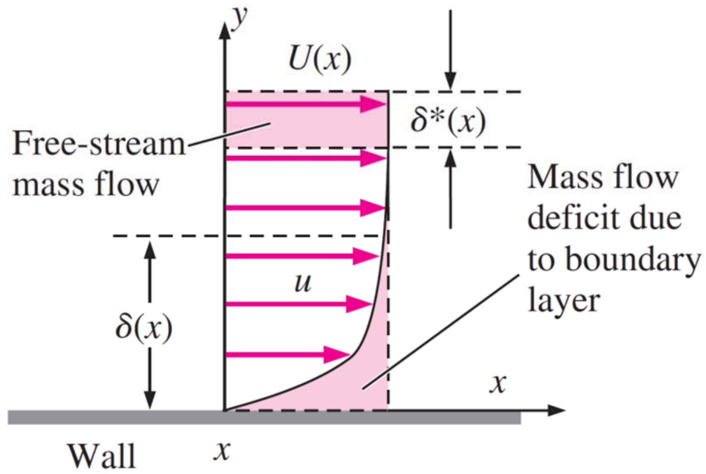

MOMENTUM THICKNESS

Momentum thickness is defined as the loss of momentum flux per unit width divided by ρU² due to the presence of the growing boundary layer.

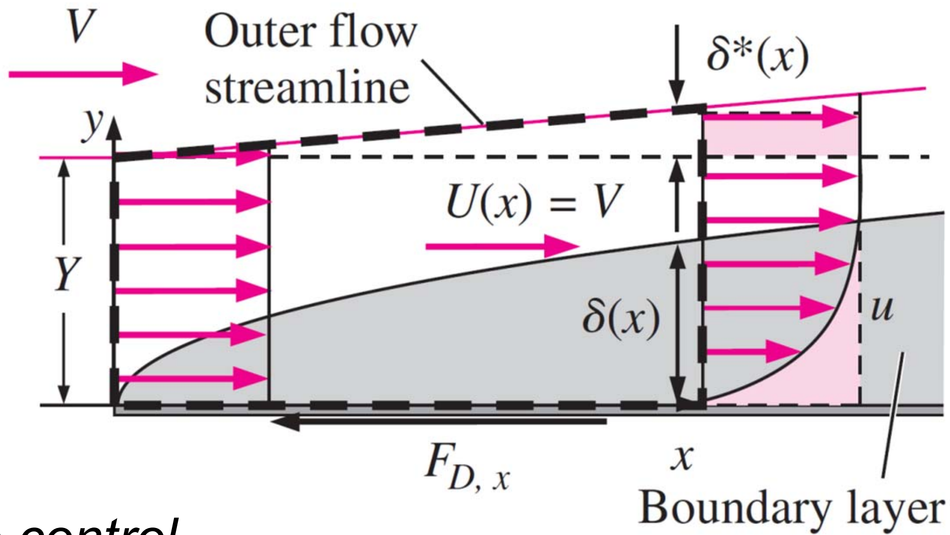

Conservation of x-momentum for the control volume:

$$\sum F_x = -F_{D,x} = \int_{CS} \rho u \vec{V} \cdot \vec{n}\, dA = \underbrace{\rho w \int_0^{Y+\delta^*} u^2\, dy}_{\text{at location } x} - \underbrace{\rho w \int_0^{Y} U^2\, dy}_{\text{at } x = 0}$$

where $F_{D,x}$ is the drag force due to friction on the plate from $x = 0$ to location x.

$$F_{D,x} = \rho w \int_0^Y u(U - u)\, dy \qquad \frac{F_{D,x}}{w} = \rho \int_0^Y u(U - u)dy \equiv \rho U^2 \theta$$

$$\theta = \int_0^\infty \frac{u}{U}\left(1 - \frac{u}{U}\right) dy$$

$$\frac{\partial u}{\partial x} + \frac{\partial v}{\partial y} = 0 \qquad u\frac{\partial u}{\partial x} + v\frac{\partial u}{\partial y} = \nu\frac{\partial^2 u}{\partial y^2}$$

$$\begin{array}{llll} u = 0 & \text{at } y = 0 & u = U & \text{as } y \to \infty \\ v = 0 & \text{at } y = 0 & u = U & \text{for all } y \text{ at } x = 0 \end{array}$$

$$\eta = y\sqrt{\frac{U}{\nu x}}$$

$$f' = \frac{u}{U} = \text{function of } \eta$$

$$2f''' + ff'' = 0 \qquad @\eta = 0,\quad f(\eta) = 0,\quad f'(\eta) = 0$$

$$@\eta \to \infty,\quad f'(\eta) = 1$$

Blasius Equation

Solution of the Blasius laminar flat plate boundary layer in similarity variables*

η	f''	f'	f	η	f''	f'	f
0.0	0.33206	0.00000	0.00000	2.4	0.22809	0.72898	0.92229
0.1	0.33205	0.03321	0.00166	2.6	0.20645	0.77245	1.07250
0.2	0.33198	0.06641	0.00664	2.8	0.18401	0.81151	1.23098
0.3	0.33181	0.09960	0.01494	3.0	0.16136	0.84604	1.39681
0.4	0.33147	0.13276	0.02656	3.5	0.10777	0.91304	1.83770
0.5	0.33091	0.16589	0.04149	4.0	0.06423	0.95552	2.30574
0.6	0.33008	0.19894	0.05973	4.5	0.03398	0.97951	2.79013
0.8	0.32739	0.26471	0.10611	5.0	0.01591	0.99154	3.28327
1.0	0.32301	0.32978	0.16557	5.5	0.00658	0.99688	3.78057
1.2	0.31659	0.39378	0.23795	6.0	0.00240	0.99897	4.27962
1.4	0.30787	0.45626	0.32298	6.5	0.00077	0.99970	4.77932
1.6	0.29666	0.51676	0.42032	7.0	0.00022	0.99992	5.27923
1.8	0.28293	0.57476	0.52952	8.0	0.00001	1.00000	6.27921
2.0	0.26675	0.62977	0.65002	9.0	0.00000	1.00000	7.27921
2.2	0.24835	0.68131	0.78119	10.0	0.00000	1.00000	8.27921

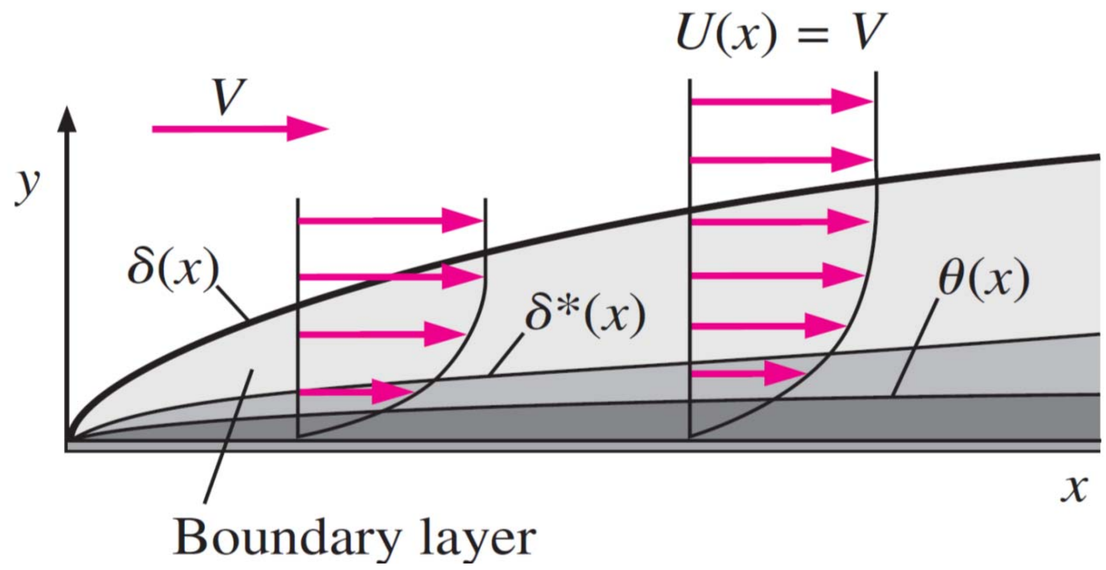

$$\boxed{\frac{\delta}{x} = \frac{4.91}{\sqrt{\mathrm{Re}_x}}} \qquad \frac{\delta^*}{x} = \frac{1.72}{\sqrt{\mathrm{Re}_x}} \qquad \frac{\theta}{x} = \frac{0.664}{\sqrt{\mathrm{Re}_x}}$$

Shape factor, $H = \dfrac{\delta^*}{\theta}$

Laminar BL, H=2.59

Turbulent BL, H=1.3-1.4

For a laminar flat plate boundary layer, displacement thickness is 35.0 percent of δ, and momentum thickness is 13.5 percent of δ.

Momentum Integral Technique

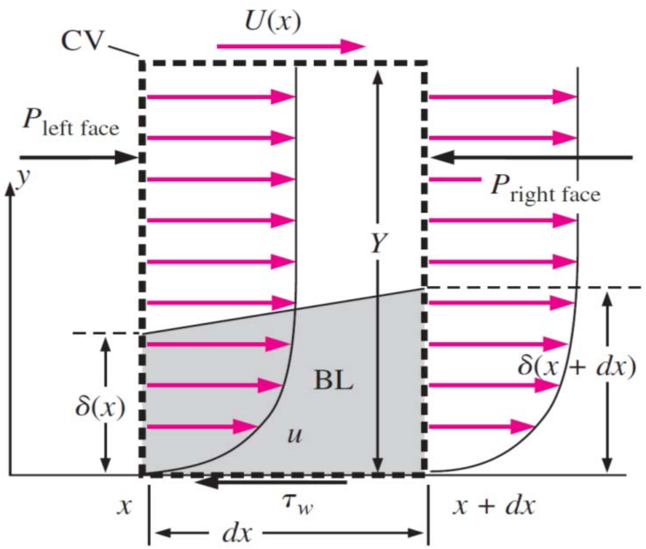

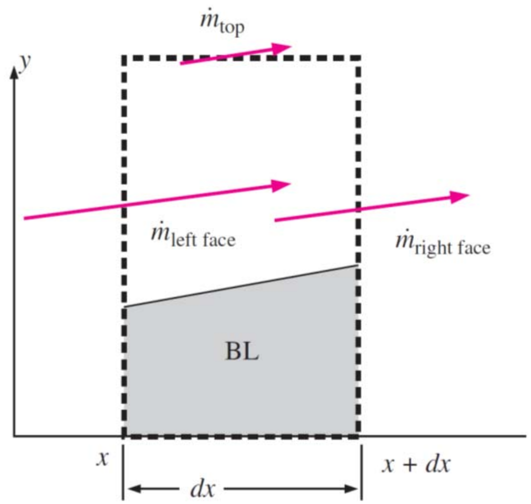

Boundary Layer Approximation: $\partial P/\partial y = 0$ $\quad P_{\text{left face}} = P$ and $P_{\text{right face}} = P + \dfrac{dP}{dx}\,dx$

$$\dot{m}_{\text{left face}} = \rho w \int_0^Y u\,dy \qquad \dot{m}_{\text{right face}} = \rho w\left[\int_0^Y u\,dy + \frac{d}{dx}\left(\int_0^Y u\,dy\right)dx\right]$$

For the case of a growing boundary layer: $\dot{m}_{\text{right face}} \ll \dot{m}_{\text{left face}}$

and mass flow from the top boundary is positive (mass flows out)

$$\dot{m}_{\text{top}} = -\rho w \frac{d}{dx}\left(\int_0^Y u\,dy\right)dx$$

The net momentum flux out of the control volume must be balanced by the force due to the shear stress acting on the control volume by the wall and the net pressure force on the control surface

The steady control volume x-momentum equation is thus

$$\underbrace{\cancel{\sum F_{x,\text{ body}}}}_{\text{ignore gravity}} + \underbrace{\sum F_{x,\text{ surface}}}_{YwP - Yw\left(P + \frac{dP}{dx}\,dx\right) - w\,dx\,\tau_w}$$

$$= \underbrace{\int_{\text{left face}} \rho u \vec{V} \cdot \vec{n}\, dA}_{-\rho w \int_0^Y u^2\,dy} + \underbrace{\int_{\text{right face}} \rho u \vec{V} \cdot \vec{n}\, dA}_{\rho w\left[\int_0^Y u^2\,dy + \frac{d}{dx}\left(\int_0^Y u^2\,dy\right)dx\right]} + \underbrace{\int_{\text{top}} \rho u \vec{V} \cdot \vec{n}\, dA}_{\dot{m}_{\text{top}} U}$$

We rewrite the equation as $-Y\dfrac{dP}{dx} - \tau_w = \rho \dfrac{d}{dx}\left(\displaystyle\int_0^Y u^2\,dy\right) - \rho U \dfrac{d}{dx}\left(\displaystyle\int_0^Y u\,dy\right)$

$$U\frac{dU}{dx}\int_0^Y dy - \frac{\tau_w}{\rho} = \frac{d}{dx}\left(\int_0^Y u^2\,dy\right) - U\frac{d}{dx}\left(\int_0^Y u\,dy\right)$$

$$\frac{d}{dx}\left(\int_0^Y u(U-u)\,dy\right) + \frac{dU}{dx}\int_0^Y (U-u)\,dy = \frac{\tau_w}{\rho}$$

$$\frac{d}{dx}\left(U^2\int_0^\infty \frac{u}{U}\left(1-\frac{u}{U}\right)dy\right) + U\frac{dU}{dx}\int_0^\infty \left(1-\frac{u}{U}\right)dy = \frac{\tau_w}{\rho}$$

Kármán integral equation

$$\boxed{\frac{d}{dx}(U^2\theta) + U\frac{dU}{dx}\,\delta^* = \frac{\tau_w}{\rho}}$$

Karman-Pohlhausen Approximate Method For Solution Of Momentum Integral Equation Over A Flat Plate

Karman-Pohlhausen Method for flow over a flat plate:

$$U_\infty^2 \frac{d\delta^{**}}{dx} + (2\delta^{**} + \delta^*) U_\infty \frac{dU_\infty}{dx} = \frac{\tau_w}{\rho}$$

For flat plate, $U_\infty = U(x) = \text{Constant}$

$$-\frac{1}{\rho}\frac{dp}{dx} = U(x)\frac{dU}{dx} = 0$$

Let us assume,

$$\frac{u}{U_\infty} = a_0 + a_1\eta + a_2\eta^2 + a_3\eta^3 + a_4\eta^4.$$

For constants to be determined using bcs.

where $\eta = \dfrac{y}{\delta}$

and $\theta = \delta^{**}$

@ $y=0$, $u=0$ or @ $\eta=0$ $\frac{u}{U_\infty}=0 \rightarrow (1)$

@ $y=0$, $\frac{1}{\rho}\frac{dp}{dx} = \nu \frac{\partial^2 u}{\partial y^2}$

For flat plate, $\frac{dp}{dx}=0$, $\frac{\partial^2 u}{\partial y^2}=0$.

i.e @ $\eta=0$, $\frac{\partial^2(u/U_\infty)}{\partial \eta^2} = 0 \rightarrow (2)$

@ $y=\delta$, $u=U_\infty$, i.e @ $\eta=1$, $\frac{u}{U_\infty}=1 \rightarrow (3)$

@ $y=\delta$, $\frac{\partial u}{\partial y}=0$, i.e @ $\eta=1$, $\frac{\partial(u/U_\infty)}{\partial\eta}=0 \rightarrow (4)$

@ $y=\delta$, $\frac{\partial^2 u}{\partial y^2}=0$, i.e, @ $\eta=1$, $\frac{\partial^2(u/U_\infty)}{\partial\eta^2}=0$ (5)

using ① $a_0 = 0$

" ② $a_2 = 0$

using ③, $a_1 + \cancel{2}a_2 + a_3 = 1$

using ④, $a_1 + 3a_3 + 4a_4 = 0$

using ⑤, $6(a_3 + 2a_4) = 0 \Rightarrow a_3 + 2a_4 = 0$

This will give, $a_0 = 0$, $a_1 = 2$, $a_2 = 0$, $a_3 = -2$, $a_4 = 1$

$$\frac{u}{U_\infty} = 2\eta - 2\eta^3 + \eta^4$$

The momentum integral eqn for a flat plate,

$$U_\infty^2 \frac{d\delta^{**}}{dx} = \frac{\tau_w}{\rho}$$

$$\delta^{**} = \int_0^{\delta} \frac{u}{U_\infty}\left(1 - \frac{u}{U_\infty}\right) dy$$

$$= \int_0^{\delta} \frac{u}{U_\infty}\left(1 - \frac{u}{U_\infty}\right) dy = \delta \int_0^1 (1 - 2\eta + 2\eta^3 - \eta^4)(2\eta - 2\eta^3 + \eta^4)\, d\eta$$

$$= \frac{37}{315}\delta$$

The wall shear stress

$$\tau_w = \mu \frac{\partial u}{\partial y}\Big|_{y=0}$$

$$= \mu \left[\frac{U_\infty}{\delta} \frac{\partial (u/U_\infty)}{\partial \eta}\right]_{\eta=0} = \mu \frac{U_\infty}{\delta} \frac{\partial}{\partial \eta}\left(2\eta - 2\eta^3 + \eta^4\right)\Big|_{\eta=0}$$

$$= \frac{2\mu U_\infty}{\delta}$$

Substituting,

$$U_\infty^2 \frac{d}{dx}\left(\frac{37}{315}\delta\right) = \frac{2\mu U_\infty}{\rho\delta}$$

$$\Rightarrow \frac{37}{315}\frac{d\delta}{dx} = \frac{2\mu}{\rho\delta U_\infty}$$

$$\Rightarrow \int \delta\, d\delta = \frac{630}{37}\frac{\nu}{U_\infty}\int dx + C$$

$$\Rightarrow \frac{1}{2}\delta^2 = \frac{630}{37}\frac{\nu x}{U_\infty} + C$$

@ $x=0$, $\delta = 0 \Rightarrow C = 0$ $\qquad \delta^2 = \frac{630\times 2}{37}\frac{\nu x}{U_\infty}$

$$\frac{1}{2}\delta^2 = \frac{630}{37}\frac{\nu x}{U_\infty}$$

$$\delta = \sqrt{\frac{1260}{37}}\sqrt{\frac{\nu x}{U_\infty}} = \frac{5.83\, x}{\sqrt{Re_x}}$$

Although the method is an approximate one, the result is astonishing accurate, being slightly higher than the exact sol^n of Blasius eq^n.

The wall shear stress,

$$C_f = \frac{\tau_w}{\frac{1}{2}\rho U_\infty^2} = \frac{0.684}{\sqrt{Re_x}}$$

marginally diff. from 0.664 of Blasius sol^n.

For third order profile: $\frac{u}{U_\infty} = a_0 + a_1\eta + a_2\eta^2 + a_3\eta^3 \Rightarrow u/U_\infty = \frac{3}{2}\eta - \frac{1}{2}\eta^3$

$$\delta/x = \frac{4.64}{\sqrt{Re_x}}$$

Blasius	Pohlhausen
$\delta^{**} = 0.664\sqrt{\frac{\nu x}{U_\infty}} = \theta$	$\delta^{**} = 0.684\sqrt{\frac{\nu x}{U_\infty}} = \theta$
$\delta^* = 1.7208\sqrt{\frac{\nu x}{U_\infty}}$	$\delta^* = 1.75\sqrt{\frac{\nu x}{U_\infty}}$
$\frac{\tau_0}{\rho U_\infty^2} = 0.332\frac{1}{\sqrt{Re_x}}$	$= 0.343\frac{1}{\sqrt{Re_x}}$

Boundary Layers with Pressure Gradients

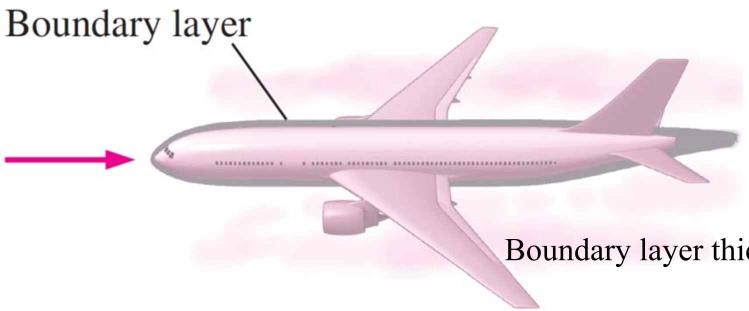

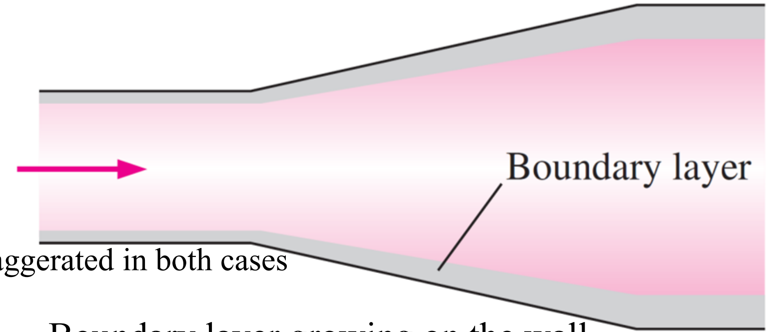

Boundary layer thickness exaggerated in both cases

Boundary layer along the fuselage of an airplane and into the wake (External Flow)

Boundary layer growing on the wall of a diffuser

Favourable pressure gradient: When the flow in the inviscid and/or irrotational outer flow region (outside of the boundary layer) accelerates, U(x) increases and $p(x)$ decreases.

Unfavourable or adverse pressure gradient: When the outer flow decelerates, U(x) decreases, $p(x)$ increases.

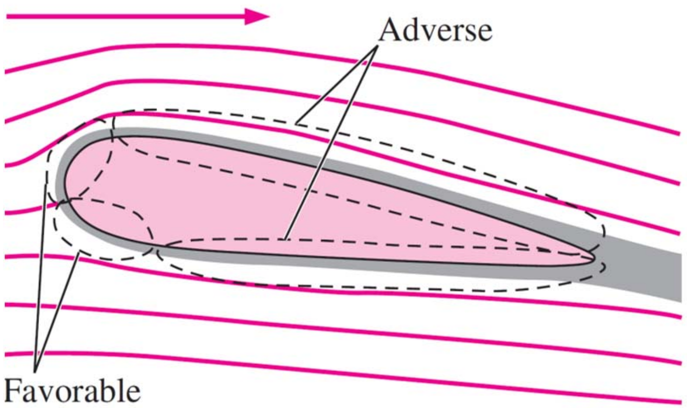

If the adverse pressure gradient is strong enough $\left(\frac{1}{\rho}\frac{dp}{dx}=U(x)\frac{dU(x)}{dx} \text{ is large}\right)$, the boundary layer is likely to **separate** off the wall.

The boundary layer equations are not valid downstream of a separation point because of reverse flow in the separation bubble.

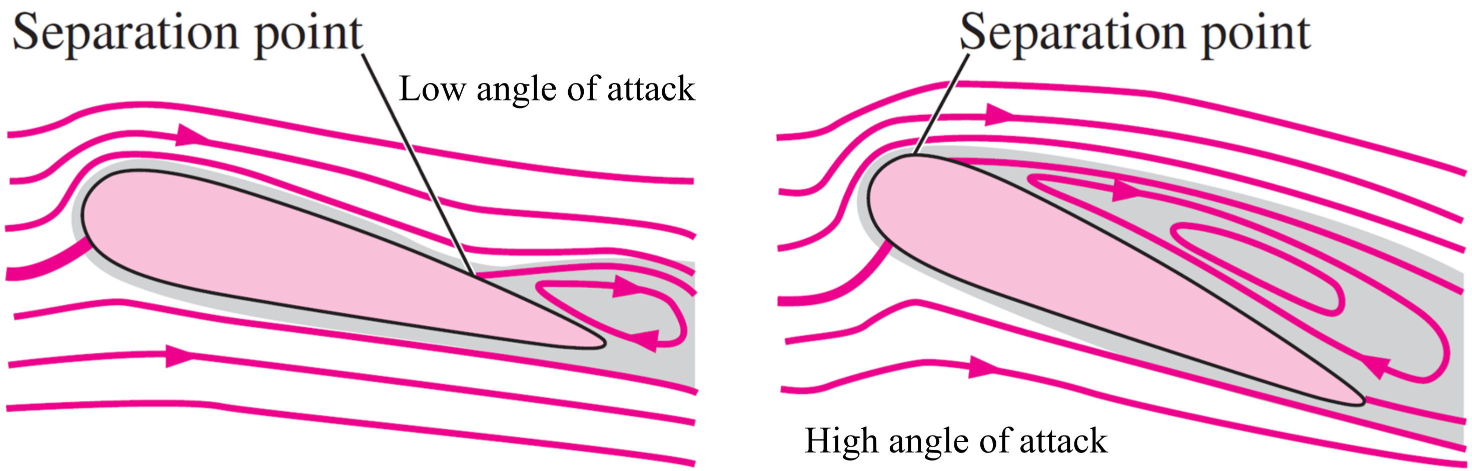

The classic case of an airfoil at too high of an angle of attack, in which the separation point moves near the front of the airfoil; the separation bubble covers nearly the entire upper surface of the airfoil-a condition known as stall.

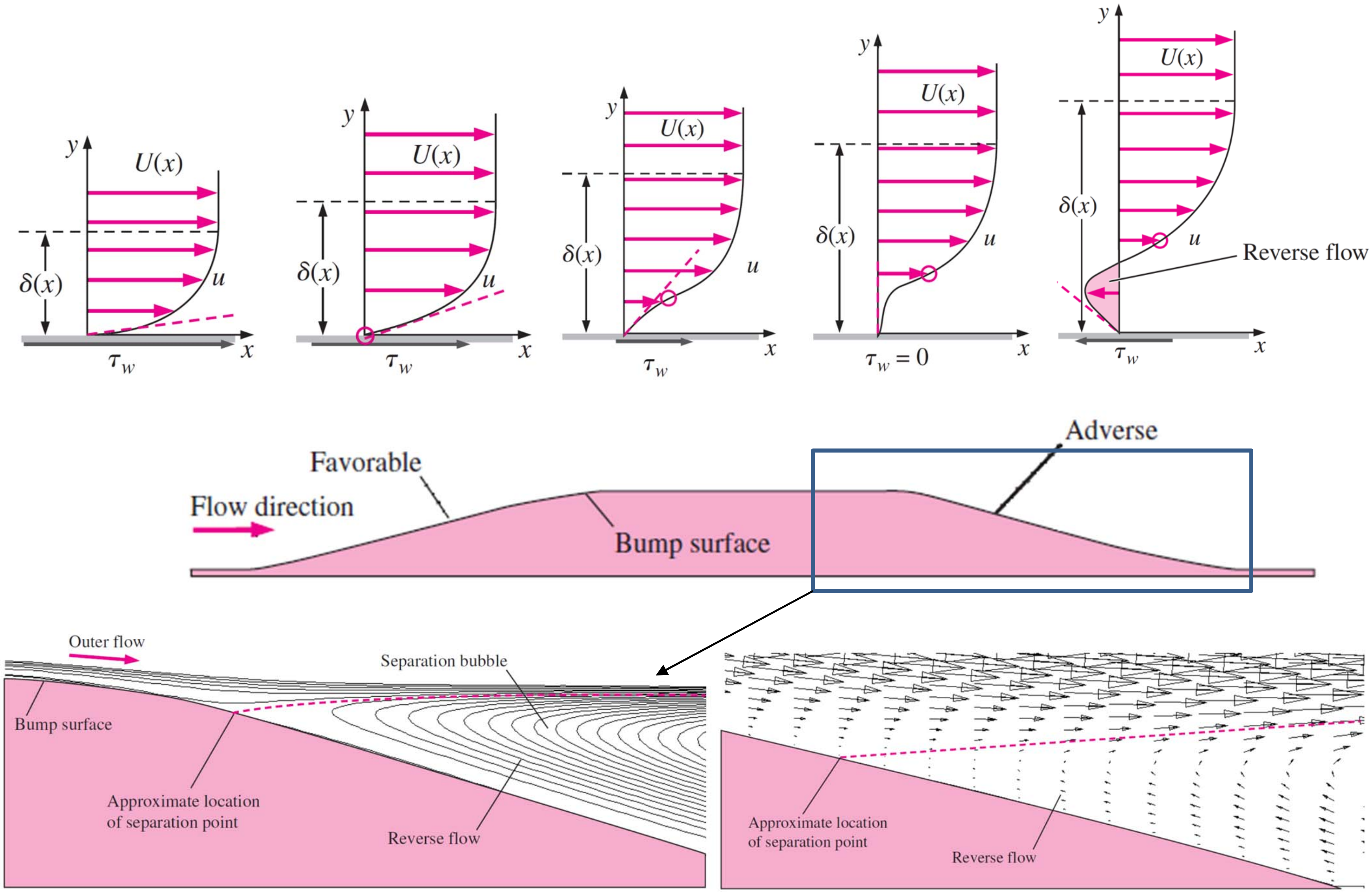

O is called PI $\Rightarrow \dfrac{\partial^2 u}{\partial y^2} = 0$

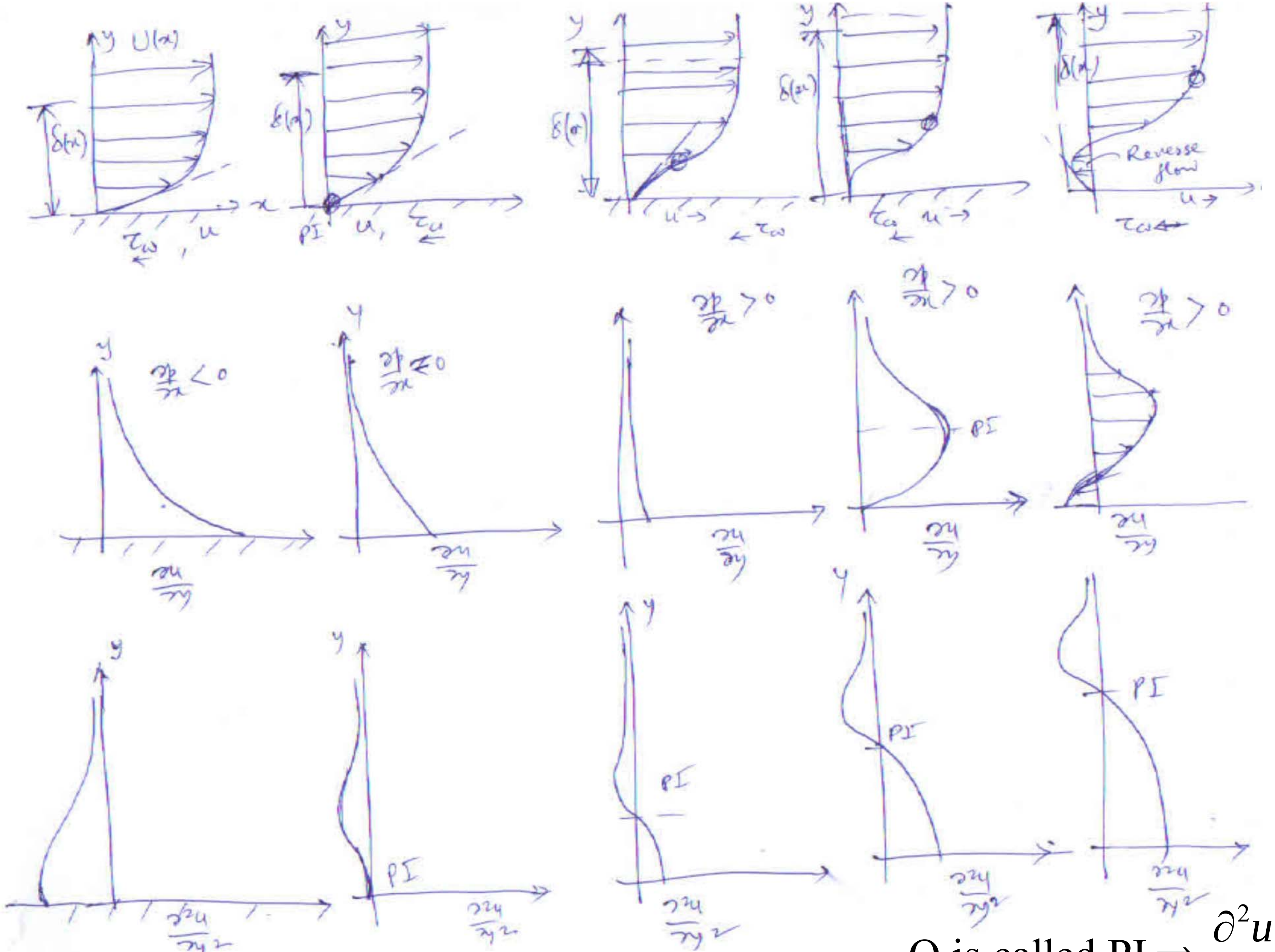

O is called PI $\Rightarrow \dfrac{\partial^2 u}{\partial y^2} = 0$

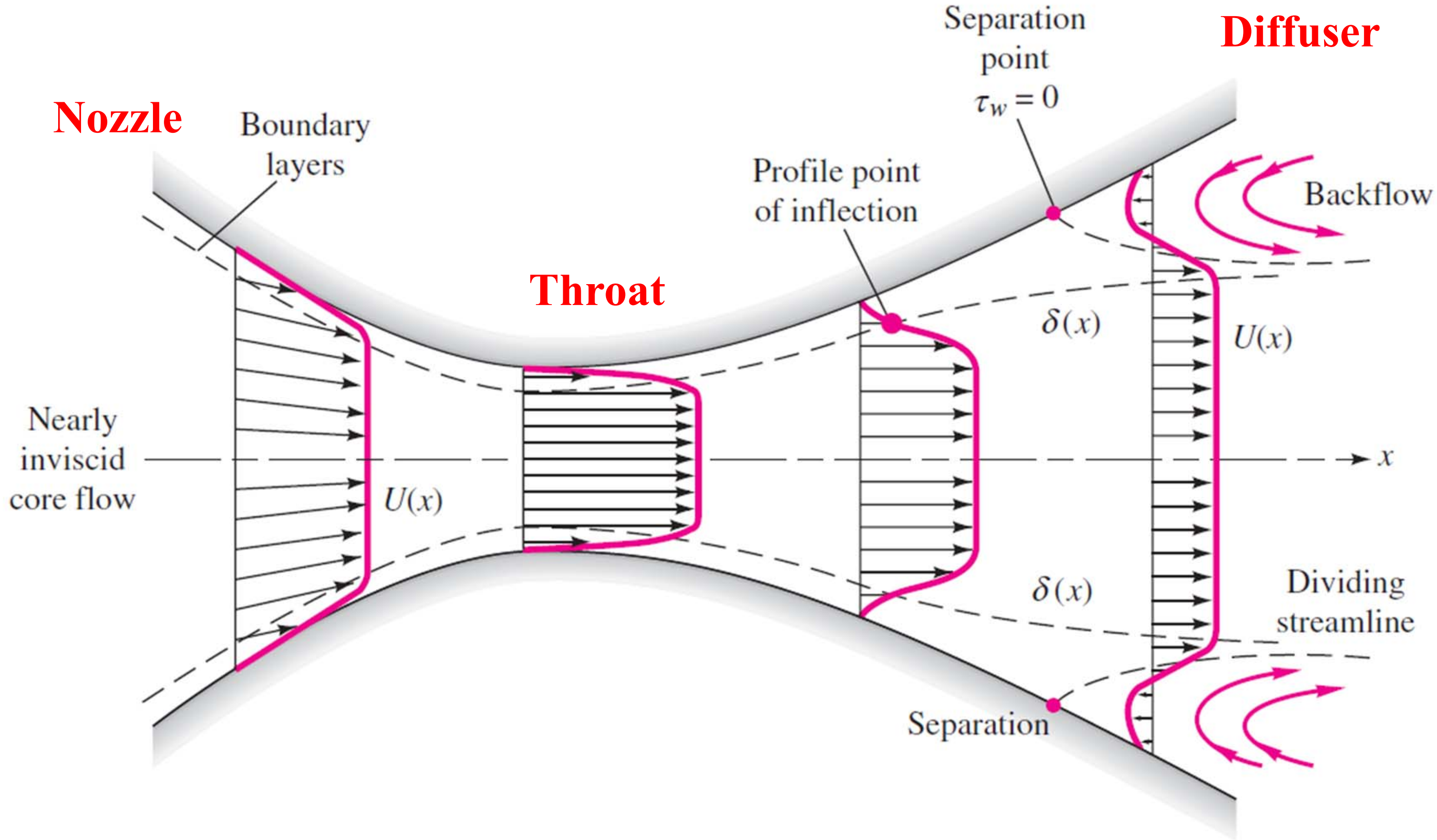

Nozzle:	*Throat*:	*Diffuser*:
Decreasing pressure and area	Constant pressure and area	Increasing pressure and area
Increasing velocity	Velocity constant	Decreasing velocity
Favorable gradient	Zero gradient	Adverse gradient (boundary layer thickens)

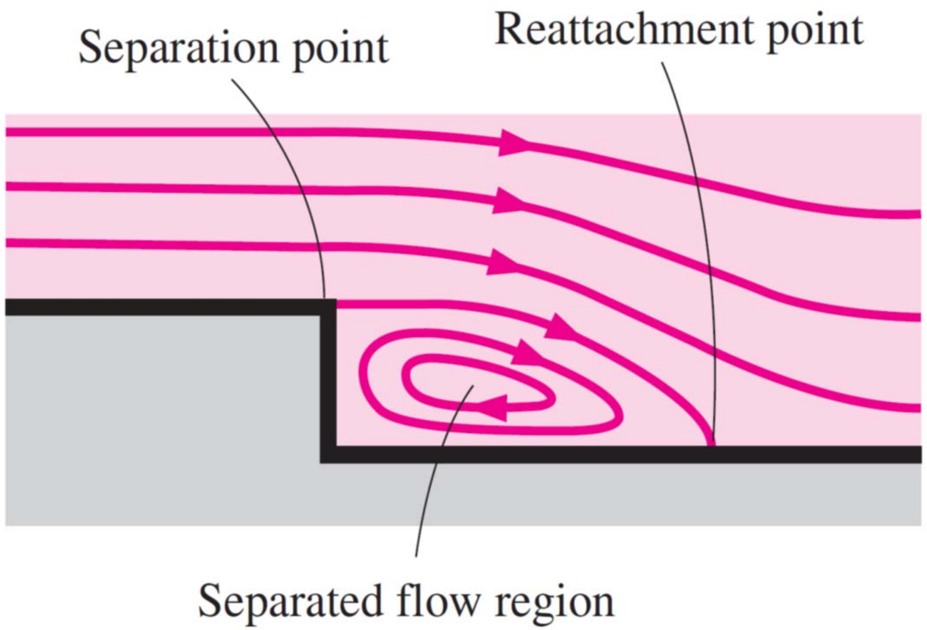
Separation point
Reattachment point
Separated flow region

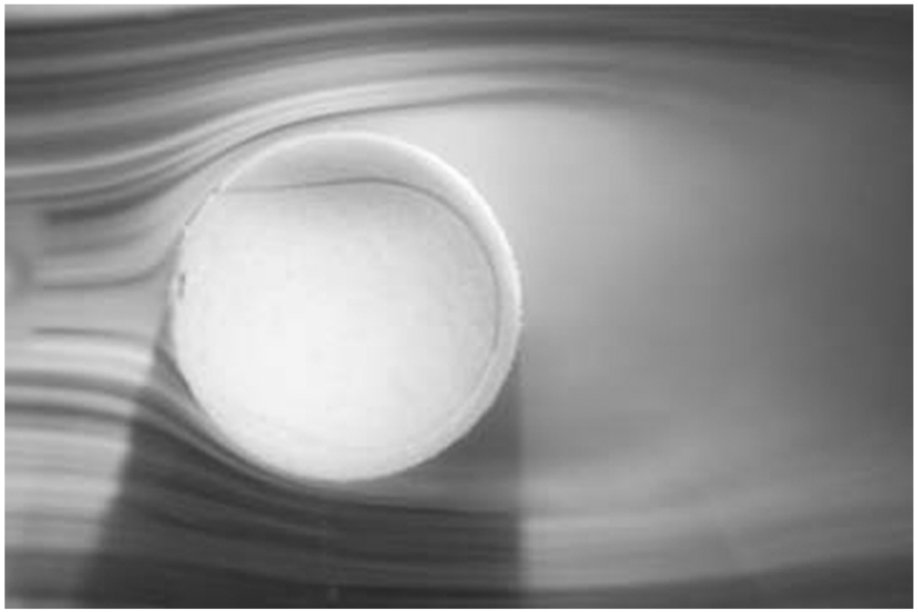

Flow Past a Circular Cylinder

Favorable
Pressure Gradient

Adverse
Pressure Gradient

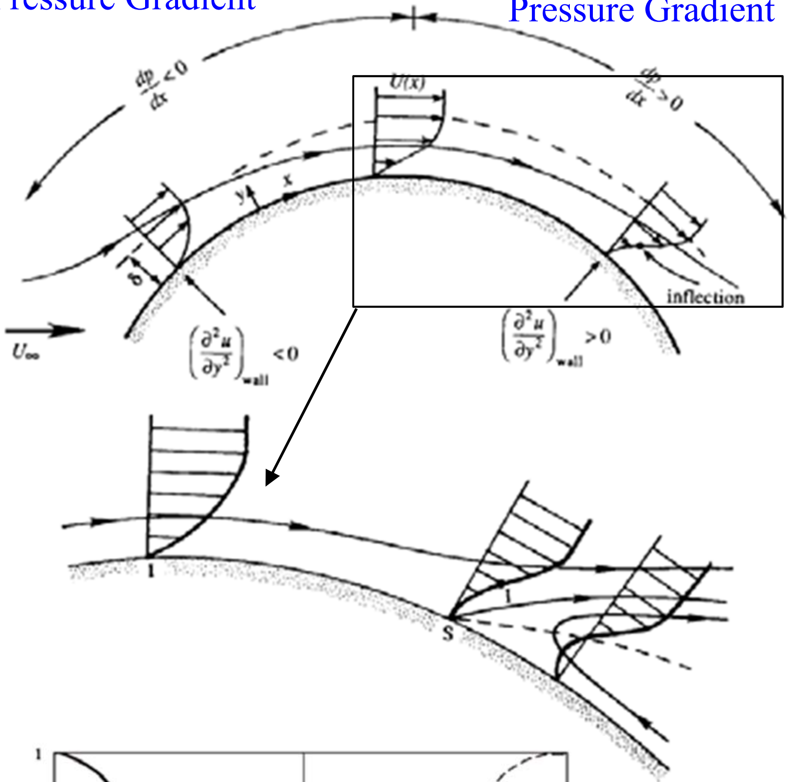

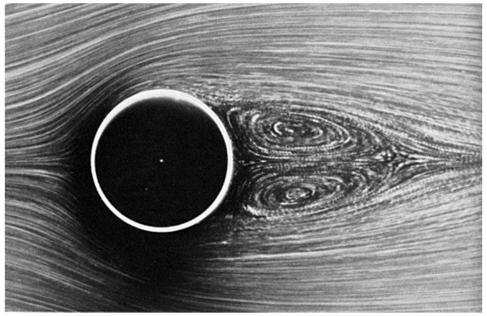

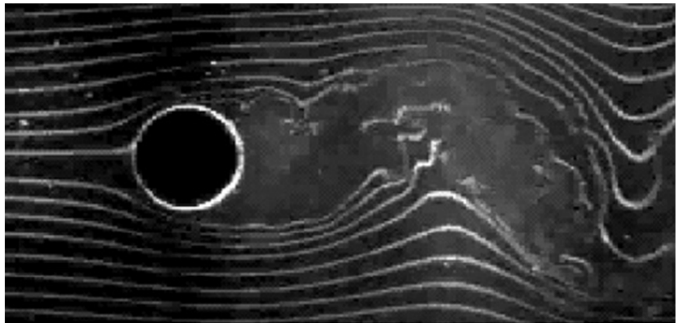

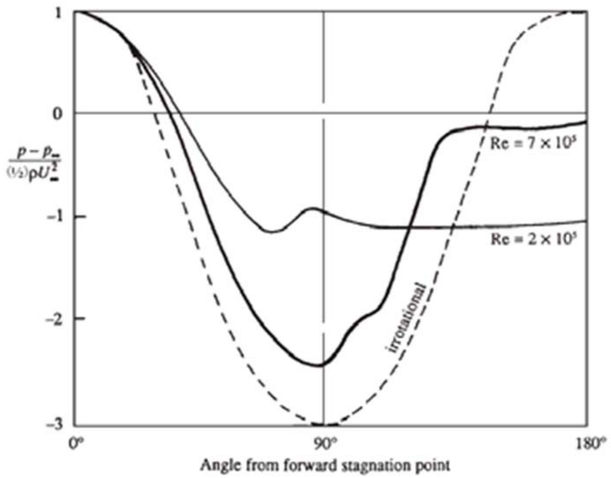

Pressure gradient plays a significant role; geometry is more important than Reynolds number

For viscous flow, adverse pressure gradient ‘overcomes’ momentum near the wall, generates inflection point in the velocity profile, may lead to separation.

Flow Past a Circular Cylinder

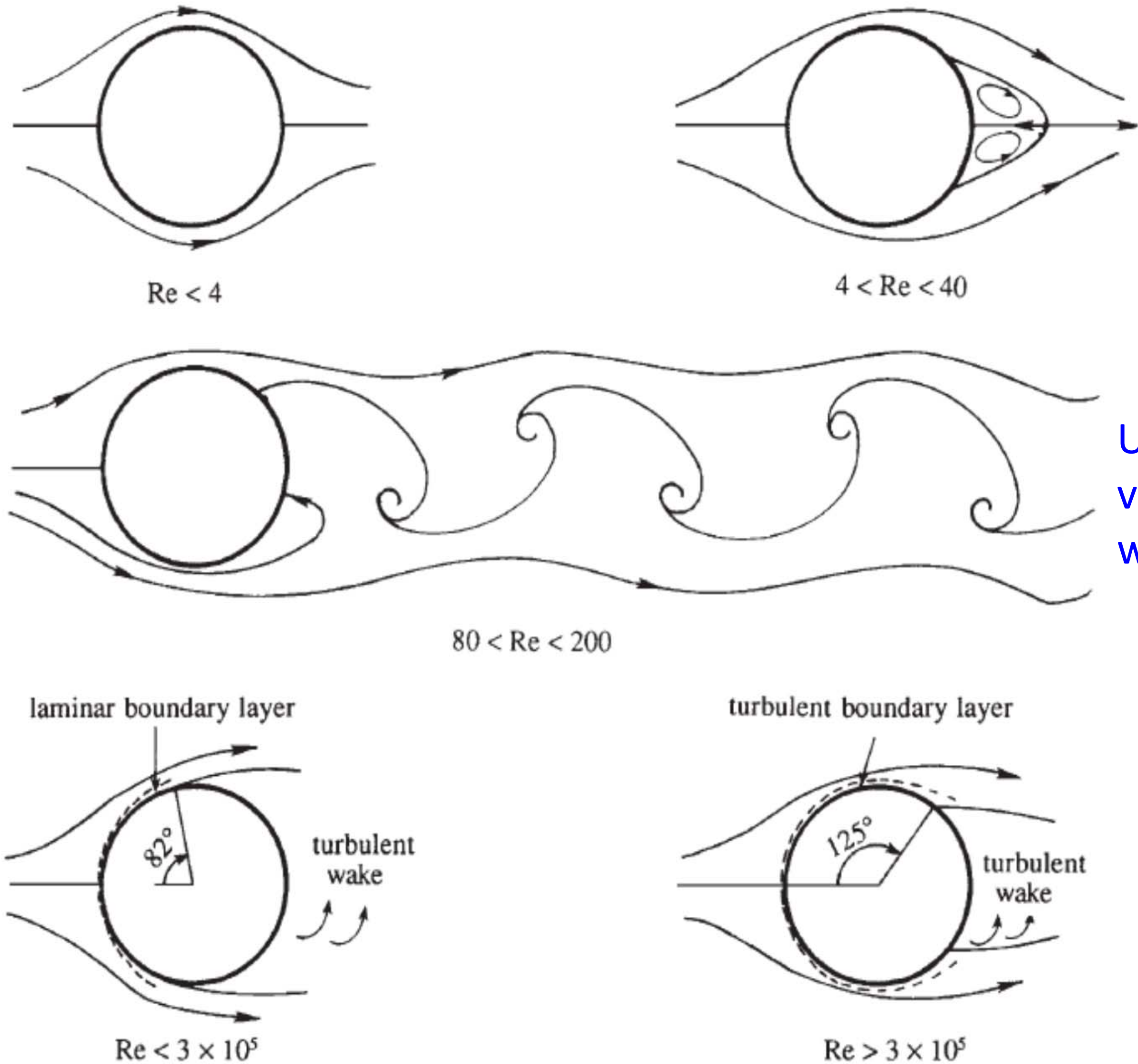

Separation starts, wake forms

Unsteady phenomena: vortex shedding in the wake

Fluid Forces Acting on Bodies

Lift and Drag Force

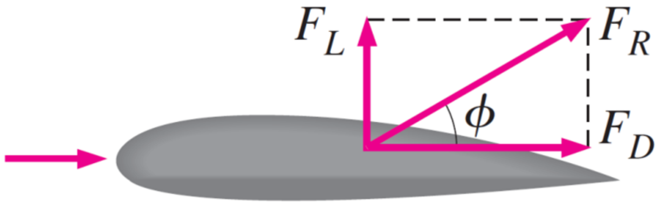

$$F_D = F_R \cos\phi$$
$$F_L = F_R \sin\phi$$

Form Drag: Because of pressure difference, Geometry dependent

Friction Drag: Because of wall shear

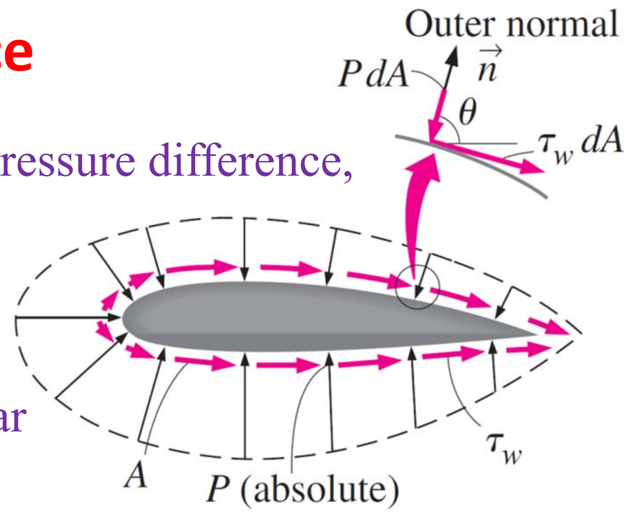

$$dF_D = \underbrace{\boxed{-P\,dA\cos\theta}}_{\text{Form drag}} + \underbrace{\boxed{\tau_w\,dA\sin\theta}}_{\text{Friction Drag}}$$

$$dF_L = -P\,dA\sin\theta - \tau_w\,dA\cos\theta$$

Drag force: $$F_D = \int_A dF_D = \int_A (-P\cos\theta + \tau_w\sin\theta)\,dA$$

Lift force: $$F_L = \int_A dF_L = -\int_A (P\sin\theta + \tau_w\cos\theta)\,dA$$

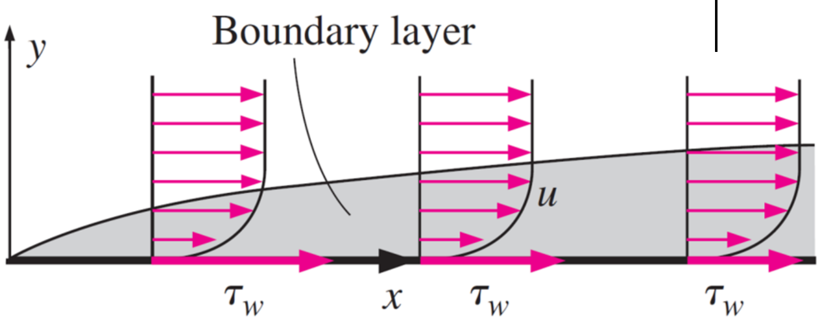

Drag force acting on a flat plate parallel to the flow depends on wall shear only.

Friction Drag

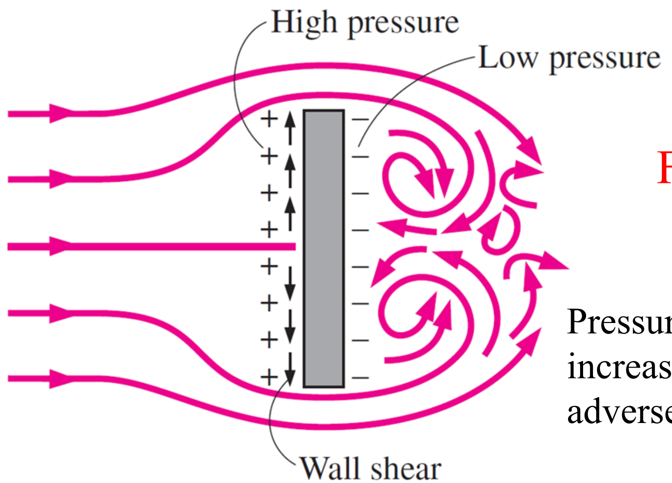

Form Drag

Pressure drag (form drag) increases; necessary condition: adverse pressure gradient

Drag force acting on a flat plate normal to the flow depends on the pressure only and is independent of the wall shear.

Drag coefficient:

$$C_D = \frac{F_D}{\frac{1}{2}\rho V^2 A}$$

Lift coefficient:

$$C_L = \frac{F_L}{\frac{1}{2}\rho V^2 A}$$

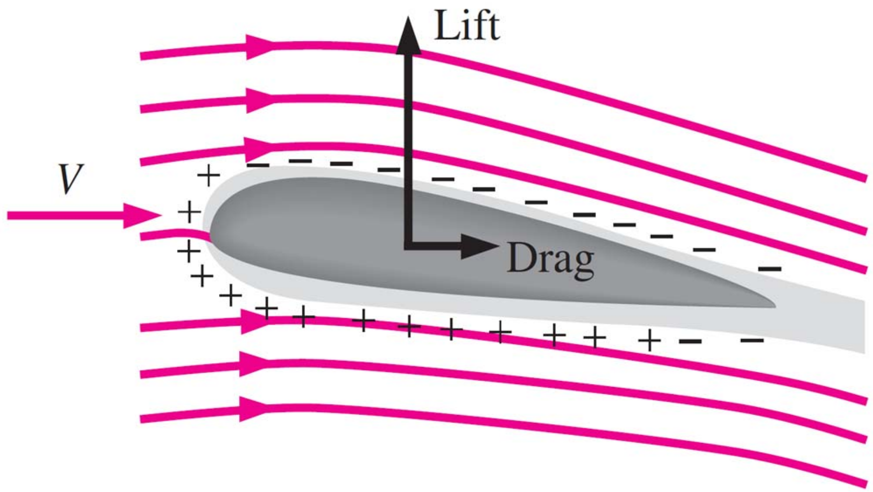

where A is ordinarily the **frontal area** (the area projected on a plane normal to the direction of flow) of the body. In other words, A is the area that would be seen by a person looking at the body from the direction of the approaching fluid. The frontal area of a cylinder of diameter D and length L, for example, is $A = LD$. In lift calculations of some thin bodies, such as airfoils, A is taken to be the **planform area,** which is the area seen by a person looking at the body from above in a direction normal to the body.

The term ρV^2 in the above equations is the dynamic pressure.

Bluff Body

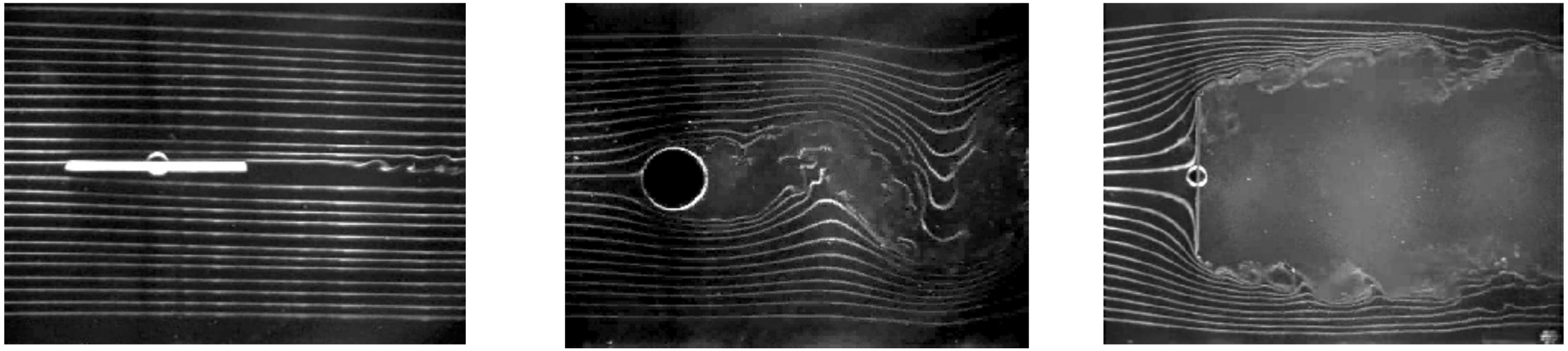

Bluffness (increasing)

Streamline Body: The pressure recovery is almost complete without or minimal separation of flow giving mostly friction drag.

Bluff Body: Beyond the point of separation, the flow reversal produces eddies. During flow past bluff-bodies, the desired pressure recovery does not take place in a separated flow and the situation gives rise to pressure drag or form drag.

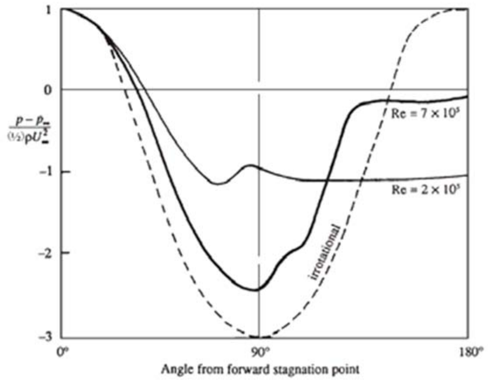

Bluff Body

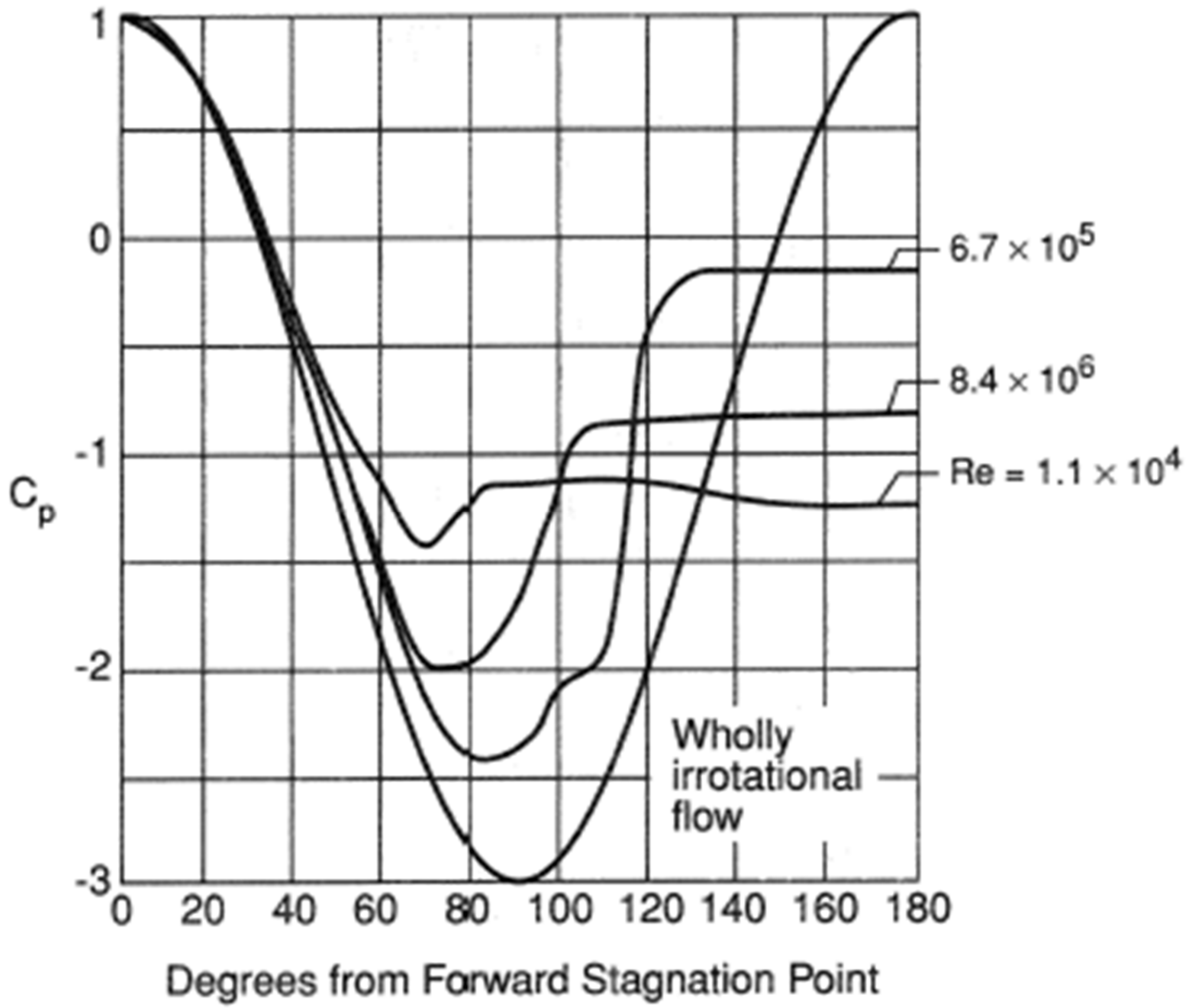

$$C_p = (p - p_\infty)/(\tfrac{1}{2}\rho U^2_\infty) = 1 - 4\sin^2\theta$$

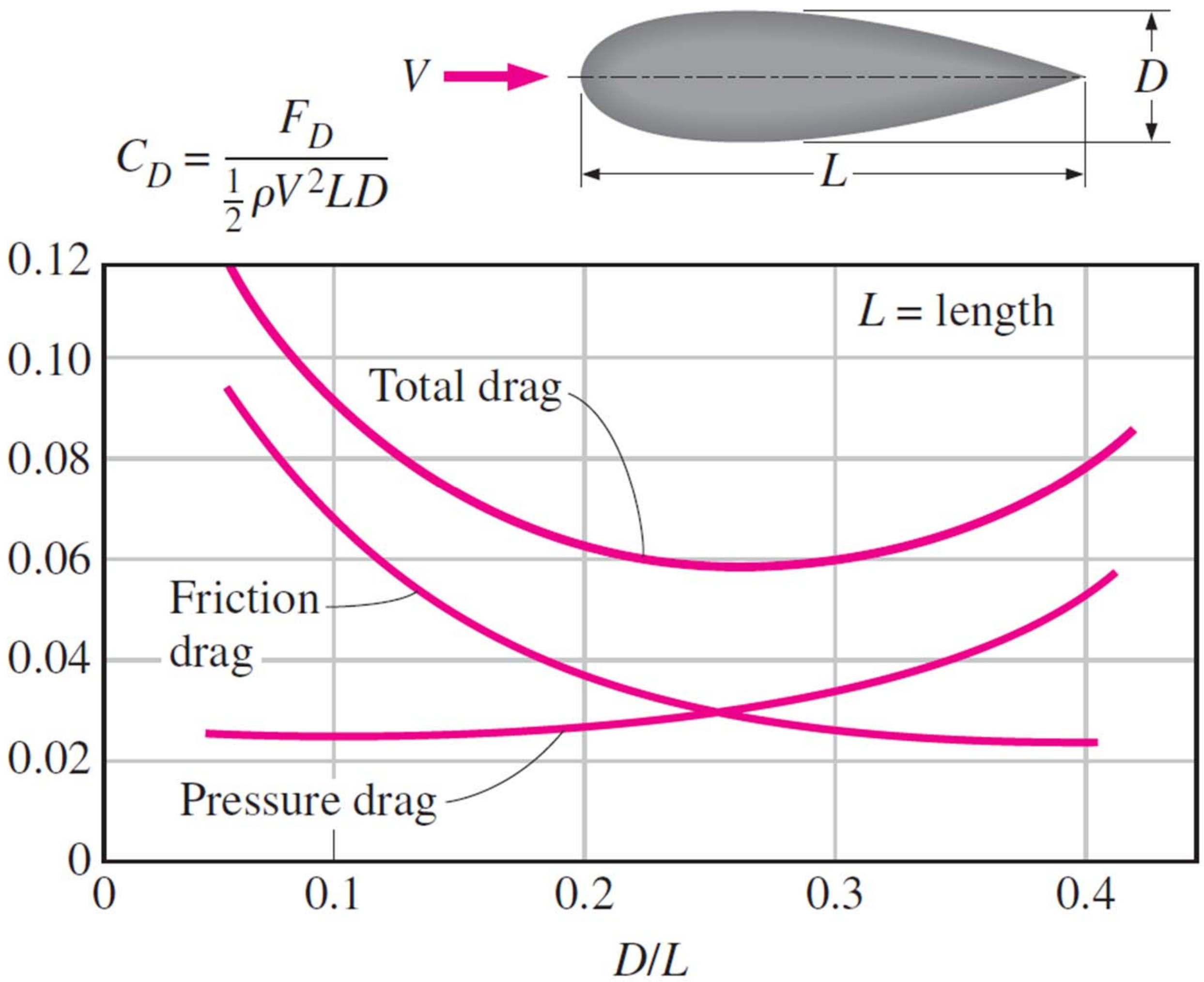

The variation of friction, pressure, and total drag coefficients of a streamlined strut with thickness-to-chord length ratio for Re $=4 \times 10^4$. Note that C_D for airfoils and other thin bodies is based on planform area rather than frontal area.

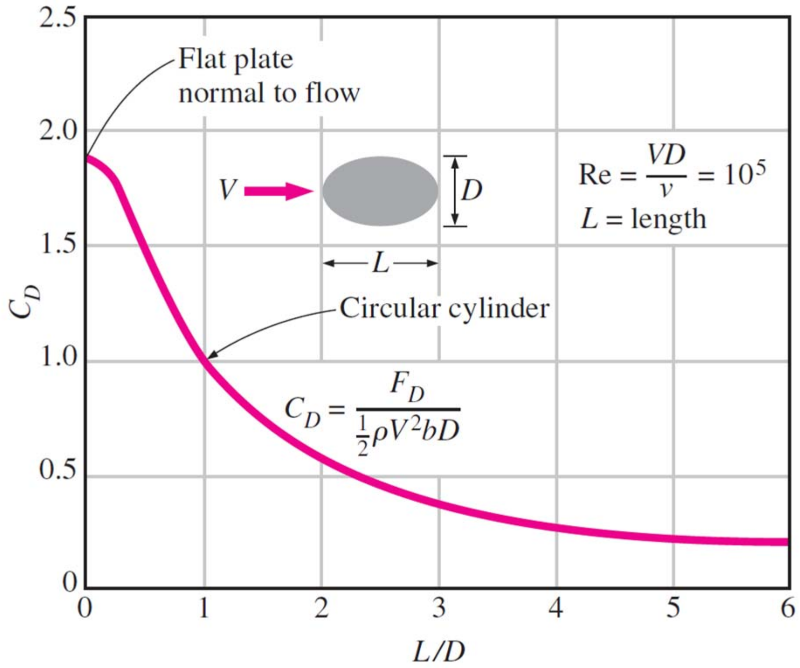

Here C_D is based on the frontal area bD where b is the width of the body.

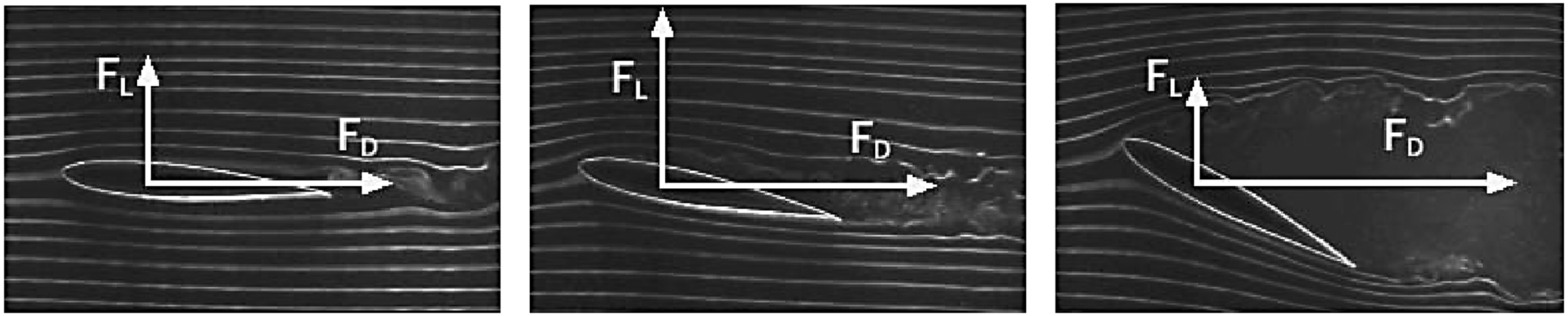

(*a*) 5° (*b*) 15° (*c*) 30°

Bluffness

At large angles of attack (usually larger than 15°), flow may separate completely from the top surface of an airfoil, reducing lift drastically and causing the airfoil to stall.

Creeping flow over a Sphere

The inertia effects are negligible in low Reynolds number flows (Re <1), called *creeping flows*, and the fluid wraps around the body smoothly.

$$C_D = \frac{24}{\text{Re}} \qquad (\text{Re} \lesssim 1)$$

$$F_D = C_D A \frac{\rho V^2}{2} = \frac{24}{\text{Re}} A \frac{\rho V^2}{2} = \frac{24}{\rho V D/\mu} \frac{\pi D^2}{4} \frac{\rho V^2}{2} = 3\pi\mu V D$$

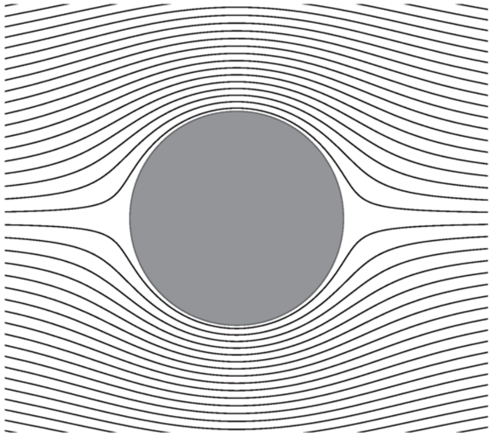

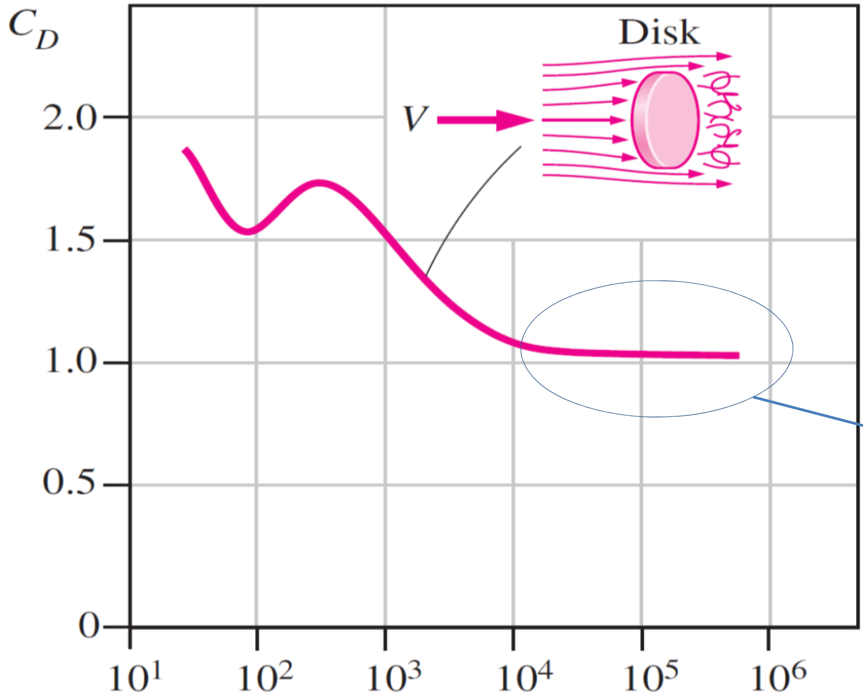

Flow over a Disk at various Reynolds Number

Independent of Re

Transition of Laminar to Turbulent BL

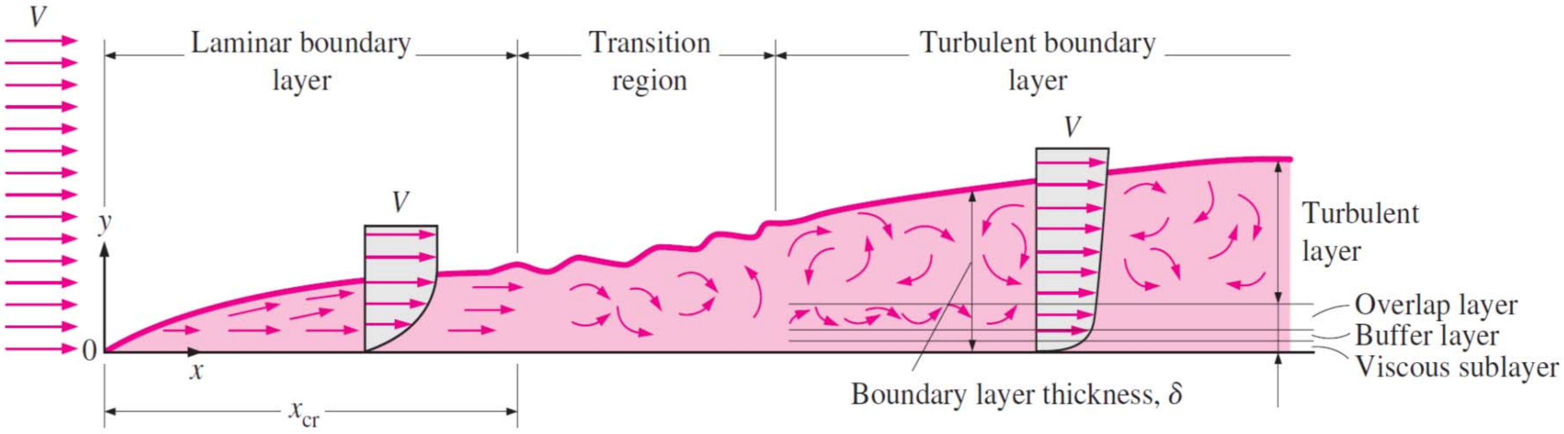

$$C_D = C_{D,\,\text{friction}} = C_f$$

$$F_D = F_f = \tfrac{1}{2} C_f A \rho V^2$$

$$\textit{Laminar:} \qquad \delta = \frac{4.91x}{\mathrm{Re}_x^{1/2}} \qquad \text{and} \qquad C_{f,\,x} = \frac{0.664}{\mathrm{Re}_x^{1/2}}, \qquad \mathrm{Re}_x < 5 \times 10^5$$

$$\textit{Turbulent:}\ \delta = \frac{0.38x}{\mathrm{Re}_x^{1/5}} \qquad \text{and} \qquad C_{f,\,x} = \frac{0.059}{\mathrm{Re}_x^{1/5}}, \qquad 5 \times 10^5 \le \mathrm{Re}_x \le 10^7$$

Empirical Turbulent flow profile: $\dfrac{u}{U} = \left(\dfrac{y}{\delta}\right)^{1/7}$

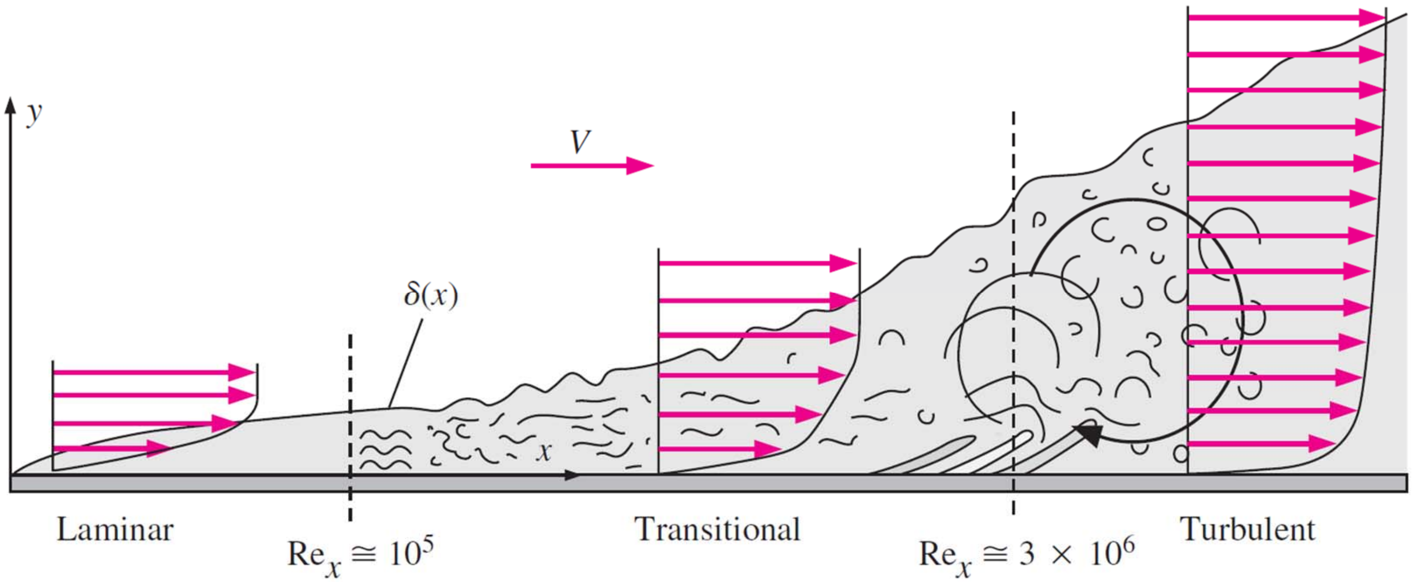

$$\frac{u}{U} = a_0 + a_1\left(\frac{y}{\delta}\right) + a_2\left(\frac{y}{\delta}\right)^2 + a_3\left(\frac{y}{\delta}\right)^3 + a_4\left(\frac{y}{\delta}\right)^4$$

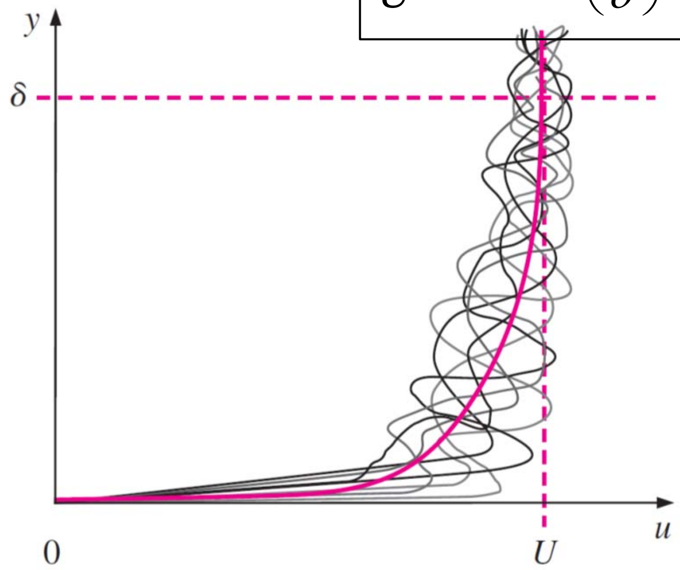

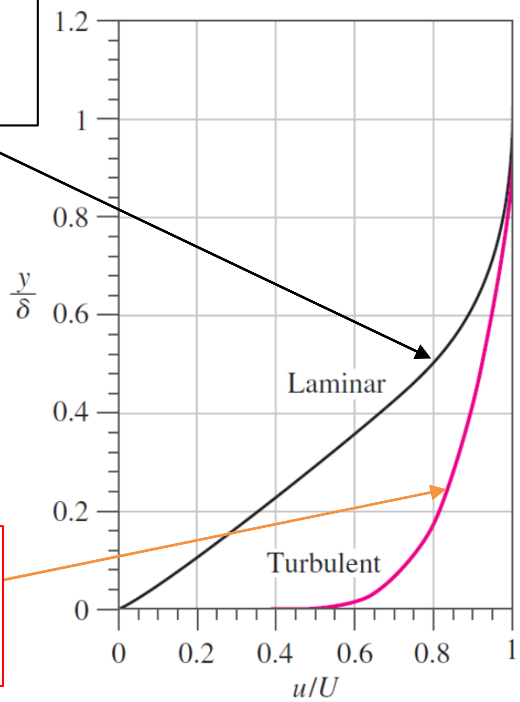

$$\frac{u}{U} = \left(\frac{y}{\delta}\right)^{1/7}$$

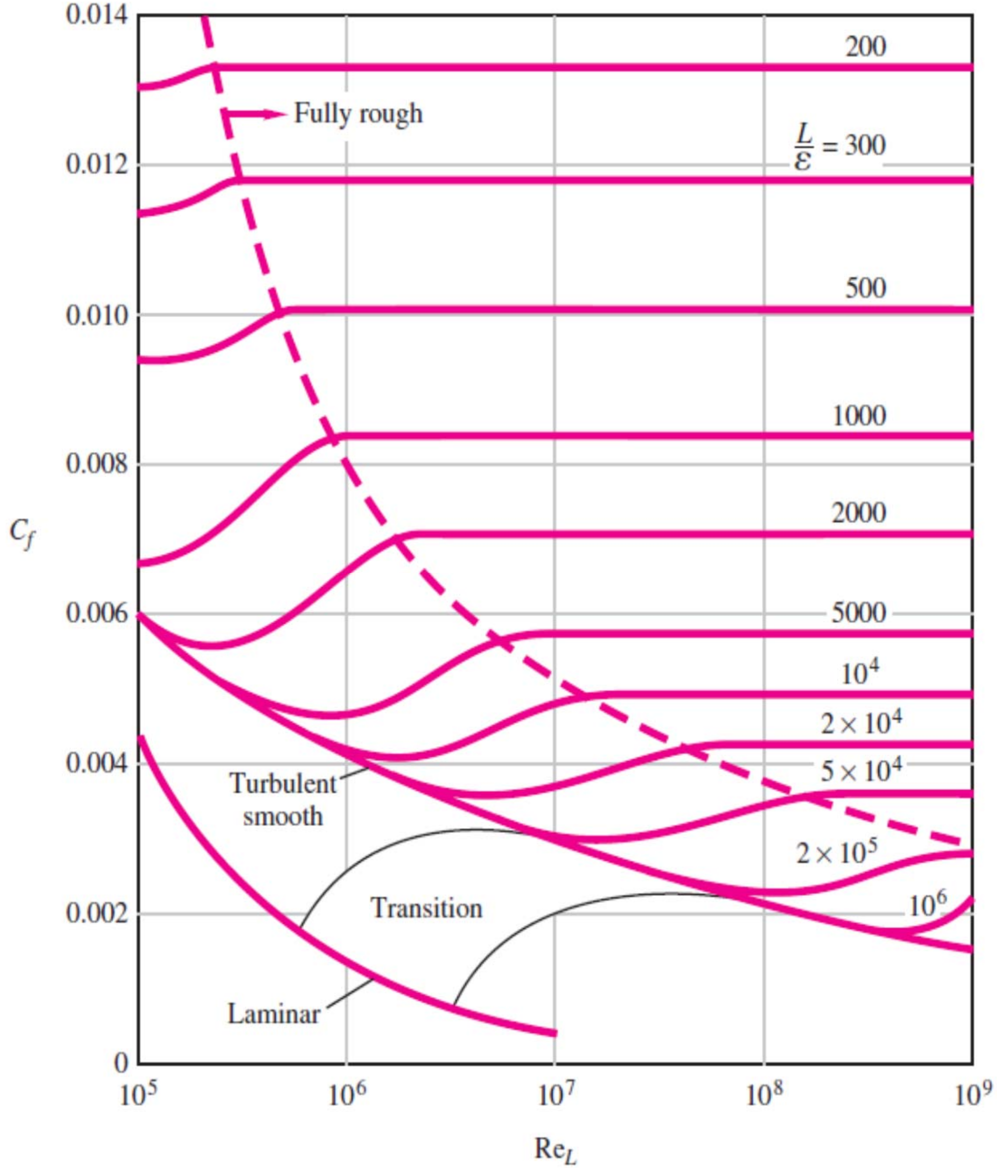

Friction coefficient for parallel flow over smooth and rough flat plates.

Flow Past a Circular Cylinder

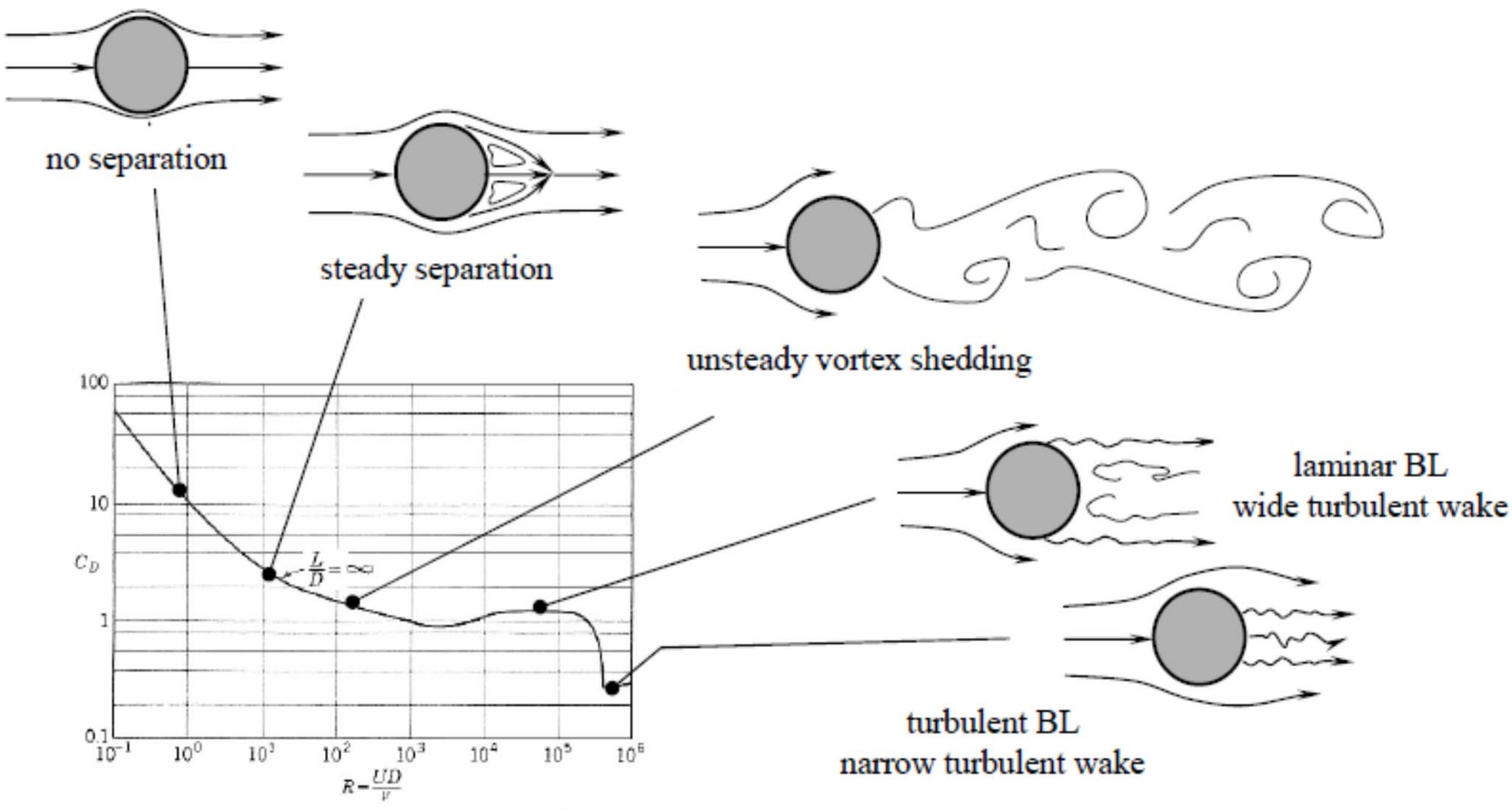

Experimentally determined drag coefficient for flow past a circular cylinder; relationship between flow structure and the drag coefficient.

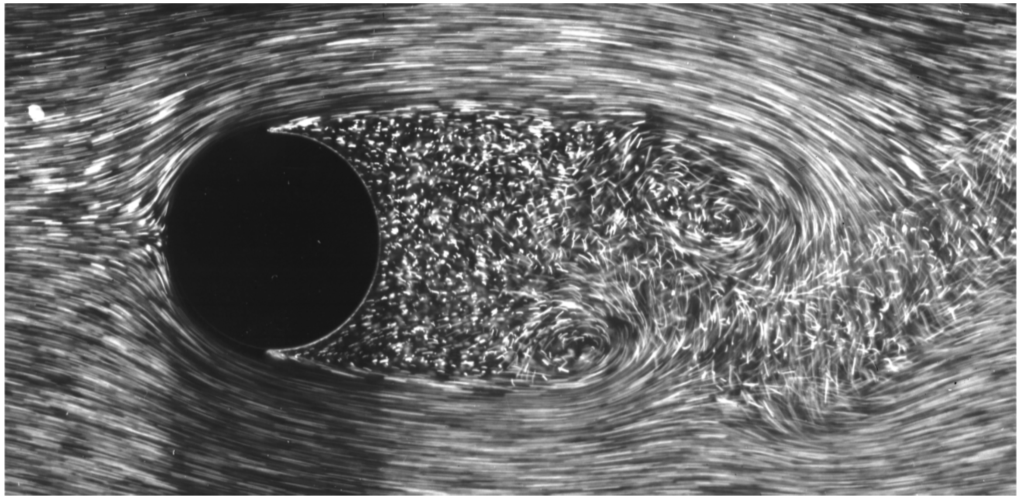

Laminar boundary layer separation with a turbulent wake; flow over a circular cylinder at Re =2000.

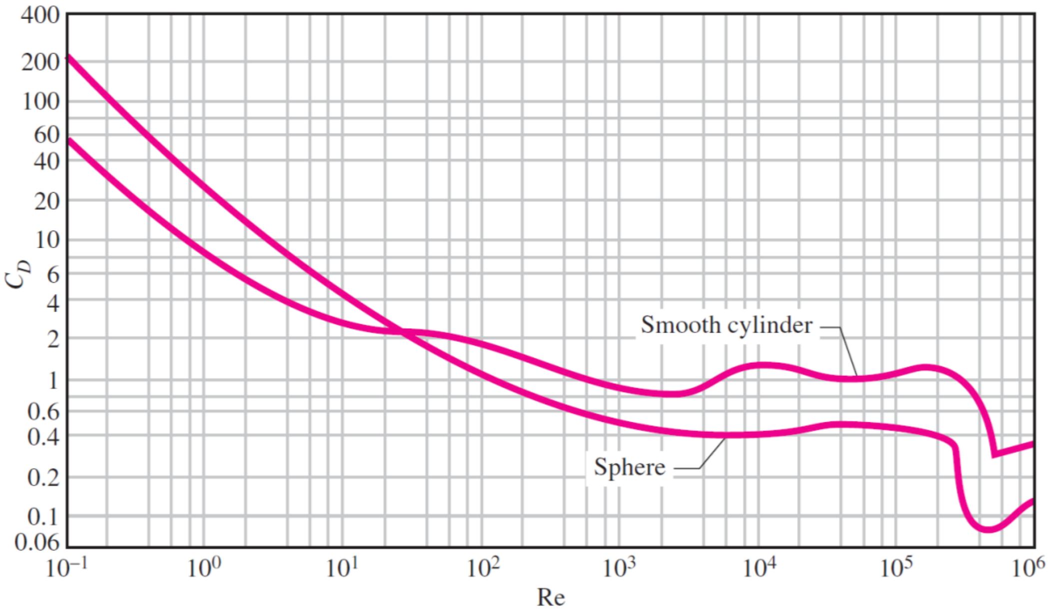

Average drag coefficient for crossflow over a smooth circular cylinder and a smooth sphere

Creeping Flow

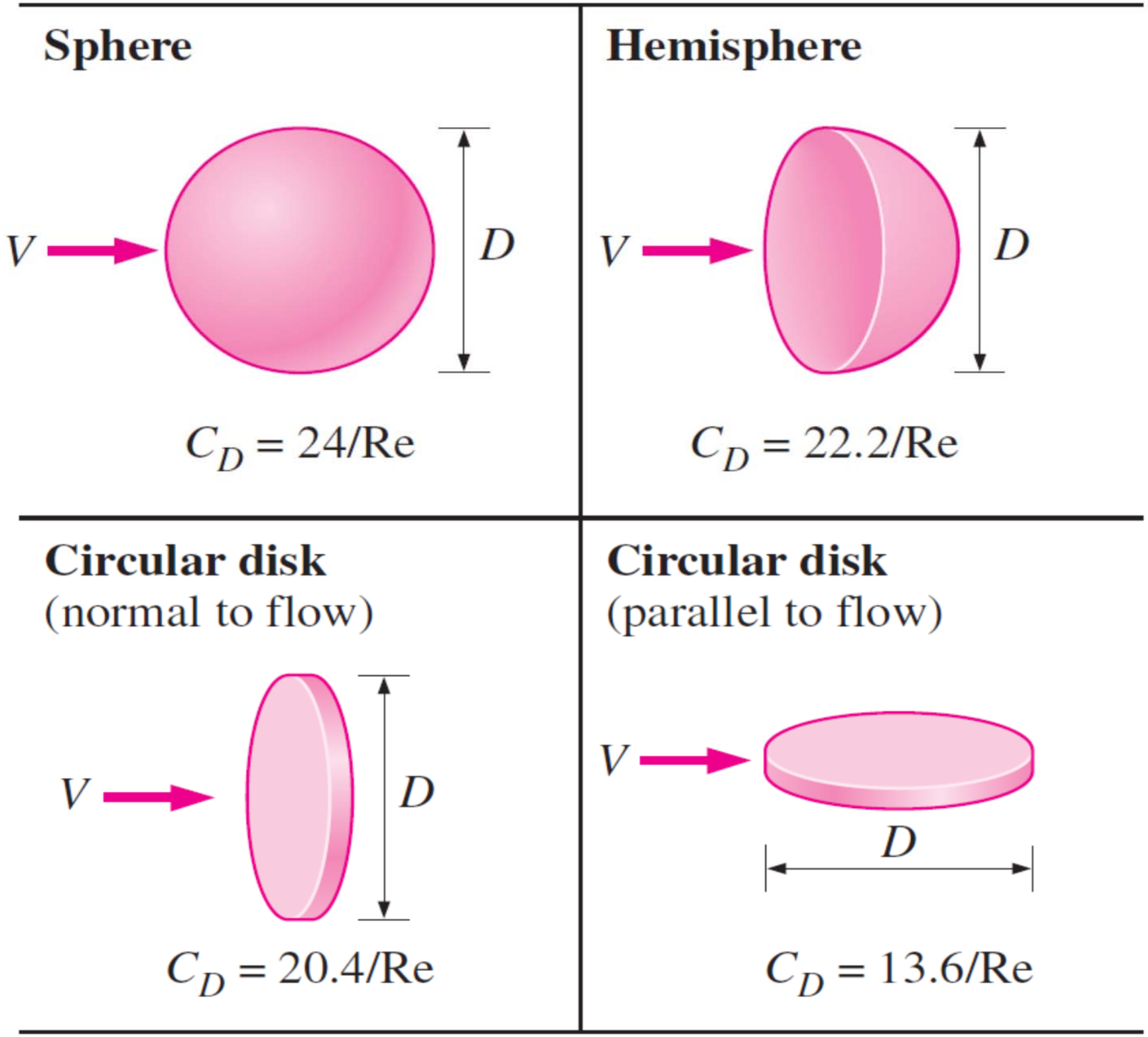

Drag coefficients C_D at low velocities (Re $\leq$ 1 where Re= VD/ν and $A=\pi D^2/4$).

Drag coefficients C_D of various two-dimensional bodies for $Re > 10^4$ based on the frontal area $A = bD$, where b is the length in direction normal to the page (for use in the drag force relation $F_D = C_D A \rho V^2/2$ where V is the upstream velocity)

Re >10^4

Square rod

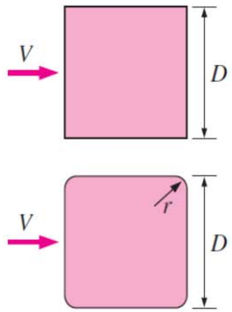

Sharp corners: $C_D = 2.2$

Round corners ($r/D = 0.2$): $C_D = 1.2$

Rectangular rod

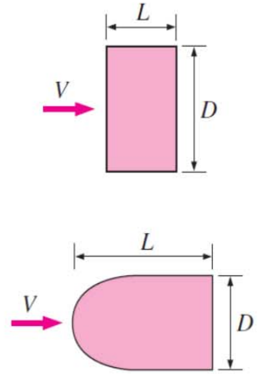

Sharp corners:

L/D	C_D
0.0*	1.9
0.1	1.9
0.5	2.5
1.0	2.2
2.0	1.7
3.0	1.3

* Corresponds to thin plate

Round front edge:

L/D	C_D
0.5	1.2
1.0	0.9
2.0	0.7
4.0	0.7

Circular rod (cylinder)

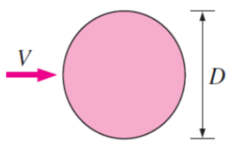

Laminar: $C_D = 1.2$

Turbulent: $C_D = 0.3$

Elliptical rod

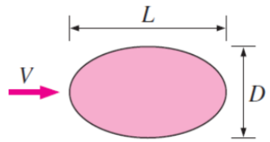

L/D	C_D Laminar	C_D Turbulent
2	0.60	0.20
4	0.35	0.15
8	0.25	0.10

Equilateral triangular rod

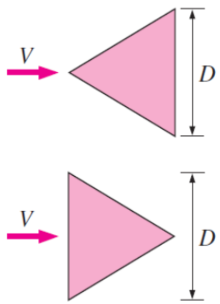

$C_D = 1.5$

$C_D = 2.0$

Semicircular shell

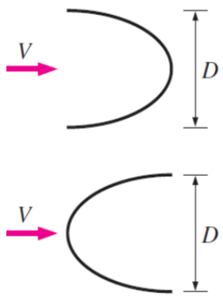

$C_D = 2.3$

$C_D = 1.2$

Semicircular rod

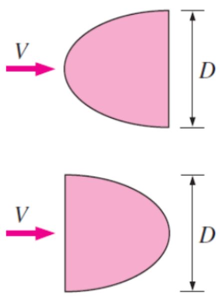

$C_D = 1.2$

$C_D = 1.7$

Representative drag coefficients C_D for various three-dimensional bodies for Re $> 10^4$ based on the frontal area (for use in the drag force relation $F_D = C_D A \rho V^2/2$ where V is the upstream velocity)

Cube, $A = D^2$

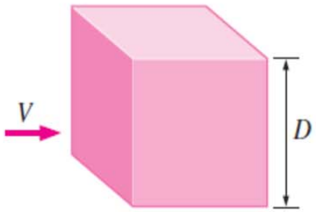

$C_D = 1.05$

Thin circular disk, $A = \pi D^2/4$

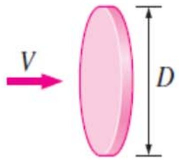

$C_D = 1.1$

Cone (for $\theta = 30°$), $A = \pi D^2/4$

$C_D = 0.5$

Re $>10^4$

Sphere, $A = \pi D^2/4$

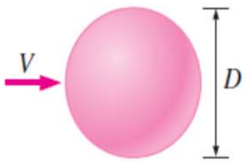

Laminar: $C_D = 0.5$

Turbulent: $C_D = 0.2$

Ellipsoid, $A = \pi D^2/4$

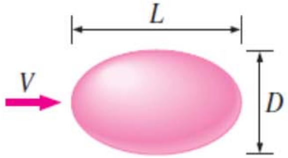

	C_D	
L/D	Laminar	Turbulent
0.75	0.5	0.2
1	0.5	0.2
2	0.3	0.1
4	0.3	0.1
8	0.2	0.1

Hemisphere, $A = \pi D^2/4$

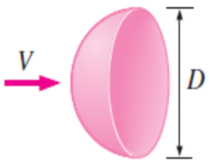

$C_D = 0.4$

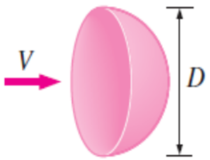

$C_D = 1.2$

Short cylinder, vertical, $A = LD$

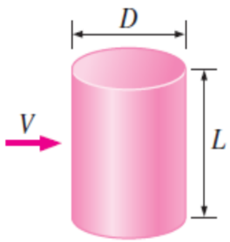

L/D	C_D
1	0.6
2	0.7
5	0.8
10	0.9
40	1.0
∞	1.2

Values are for laminar flow

Short cylinder, horizontal, $A = \pi D^2/4$

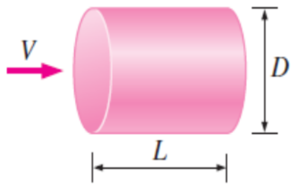

L/D	C_D
0.5	1.1
1	0.9
2	0.9
4	0.9
8	1.0

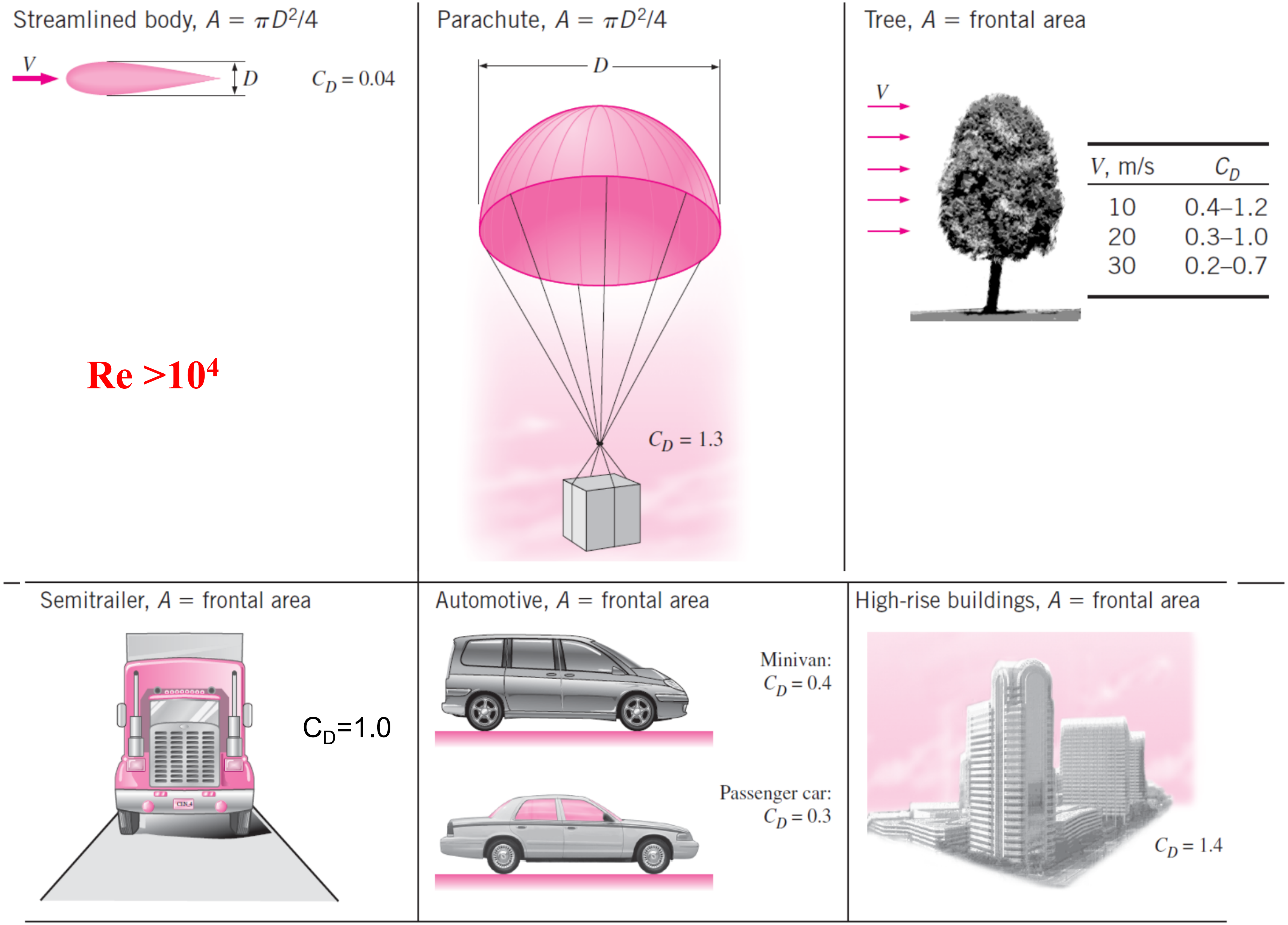

Drag Coefficient in car: 0.7 in 1940 to 0.3 in 2010

Effect of Orientation

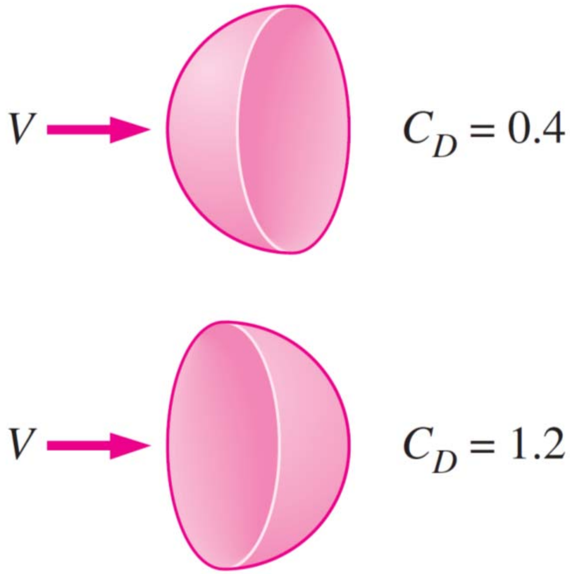

A hemisphere at two different orientations for Re > 10^4

The drag coefficient of a body may change drastically by changing the body's orientation (and thus shape) relative to the direction of flow.

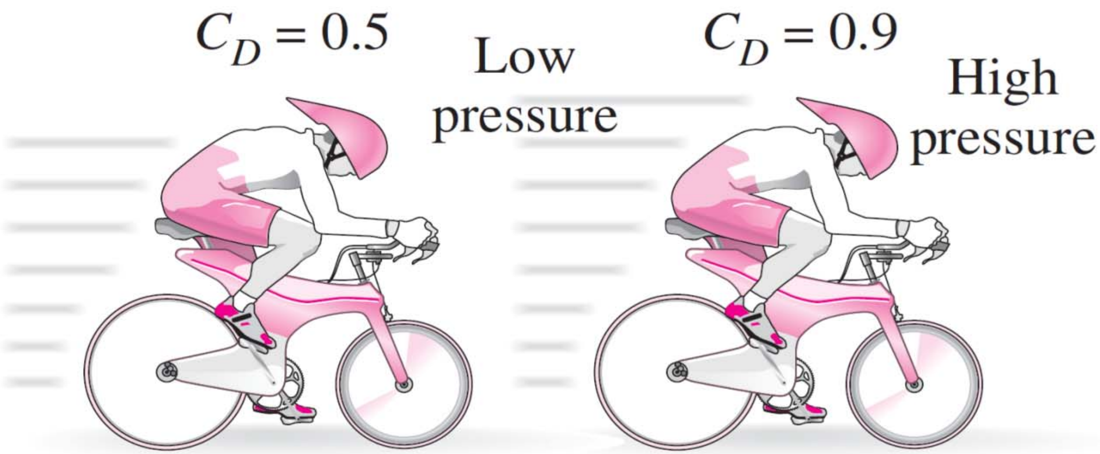

Drafting (i.e., falling into the low pressure region created by the body in front).

Effect of Surface Roughness

Sports ball aerodynamics: Tennis and Soccer

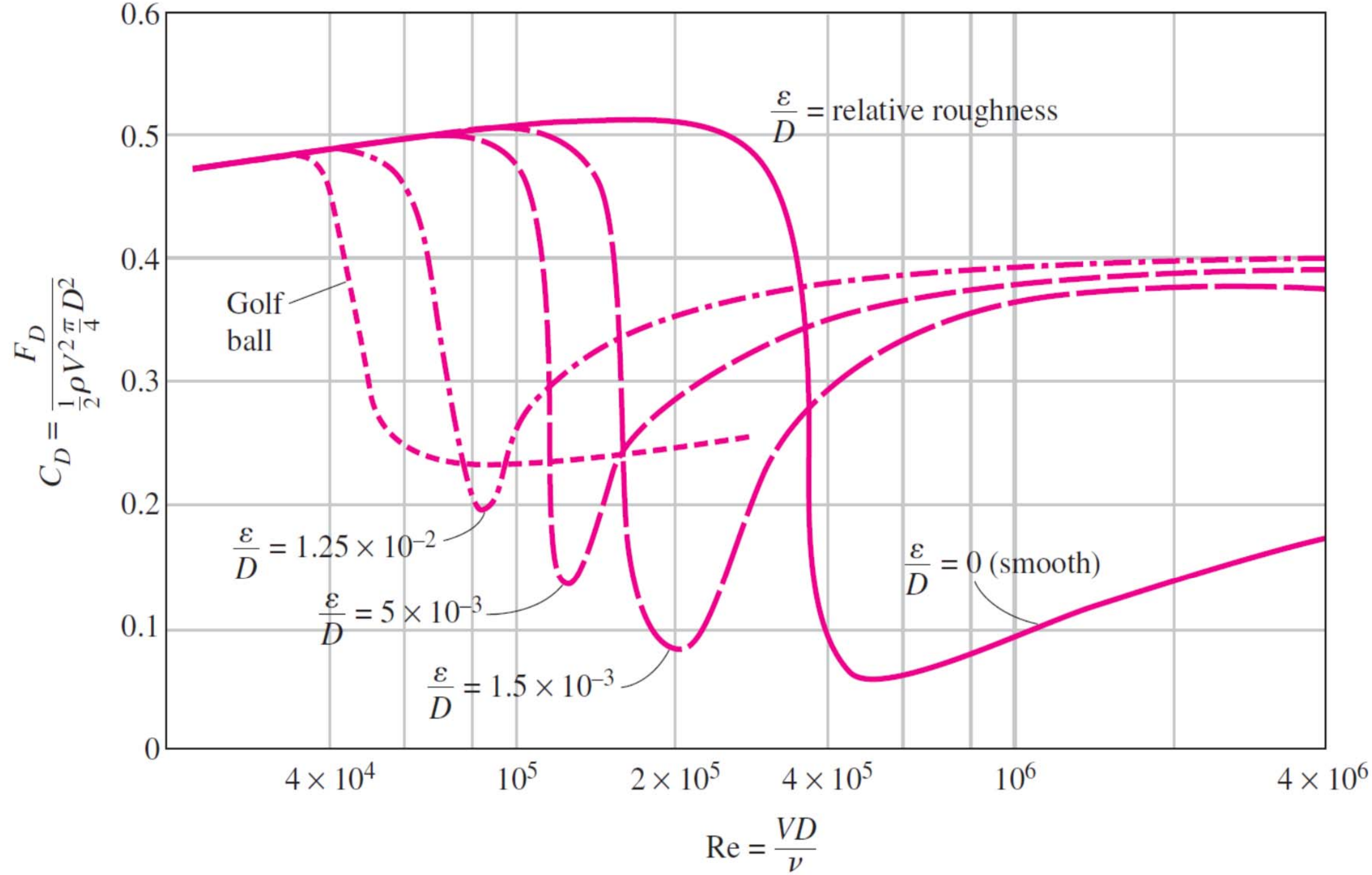

The effect of surface roughness on the drag coefficient of a sphere.

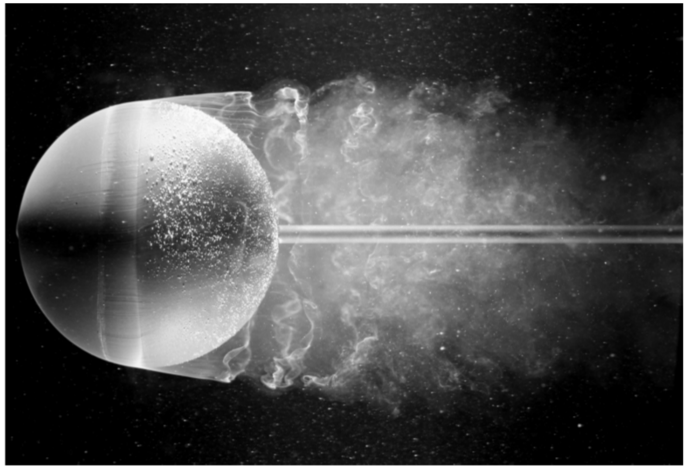

A smooth sphere at Re=15,000

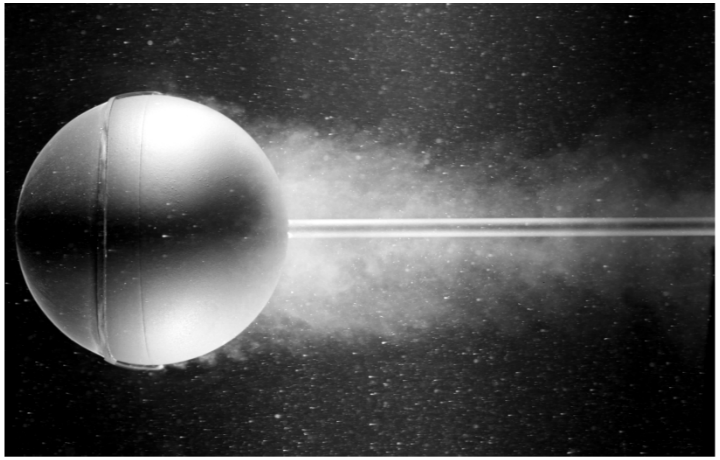

A sphere at Re=30,000 with a trip wire.

Swings of tennis/soccer ball are induced by the spin

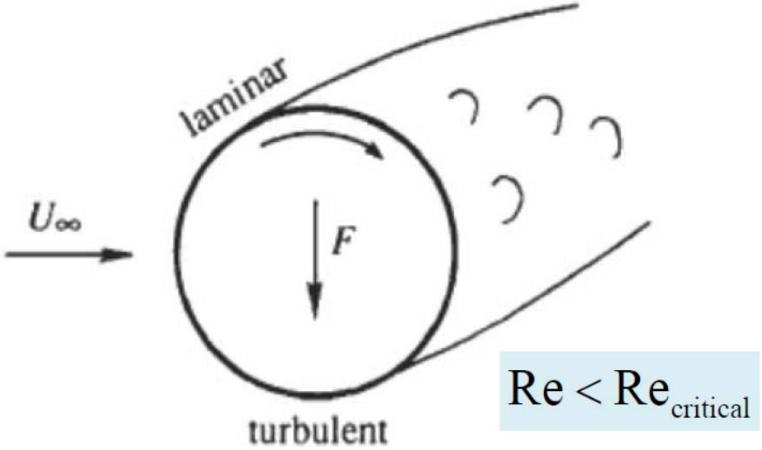

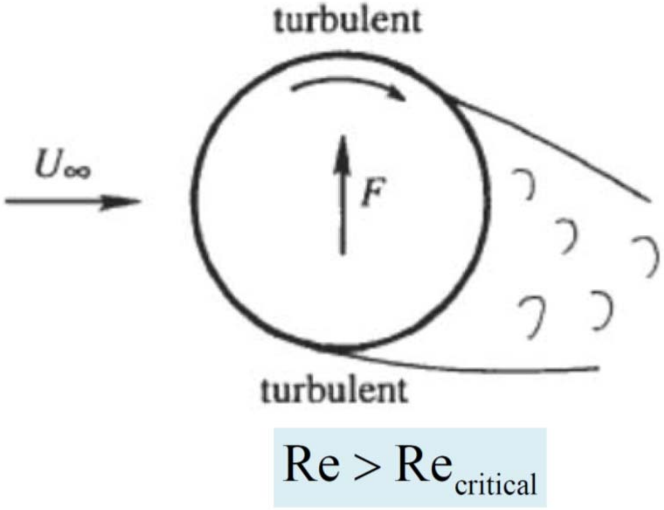

Drag Force on Swimmers

Small drag in streamlined position

Large drag in unstreamlined position

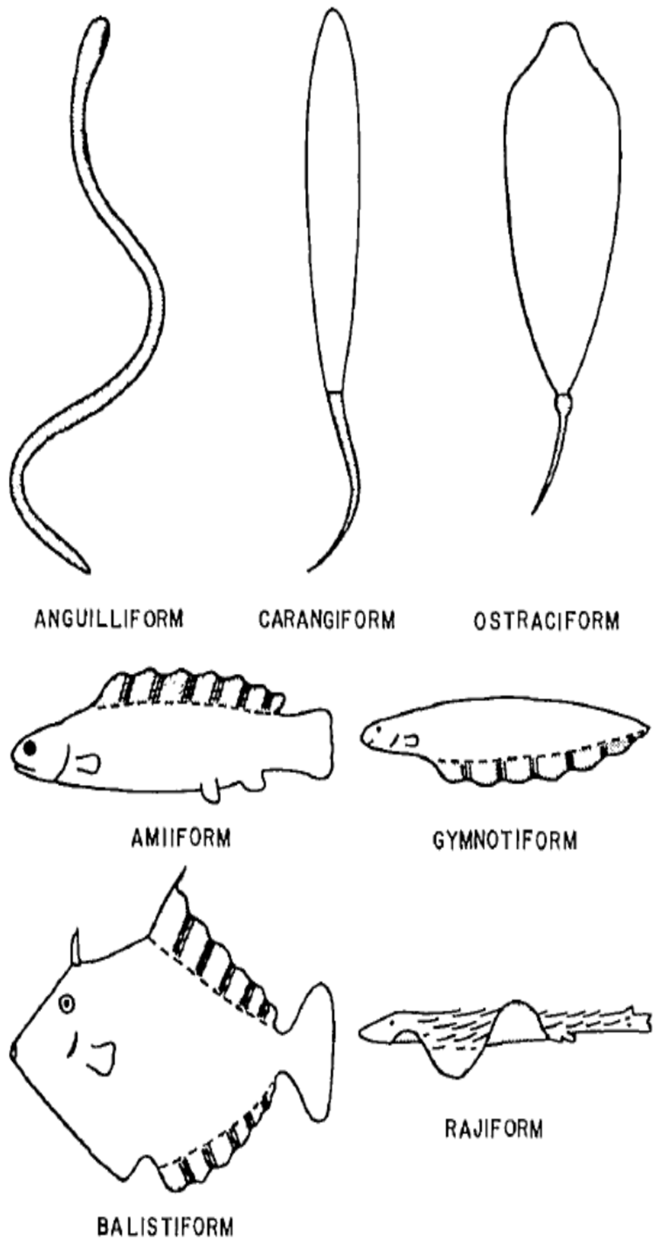

Some principal types of swimming modes in fish.

Fish Locomotion